Acta Pharmaceutica Sinica B 2025;15(2):834–851

Chinese Pharmaceutical Association
Institute of Materia Medica, Chinese Academy of Medical Sciences

Acta Pharmaceutica Sinica B

www.elsevier.com/locate/apsb
www.sciencedirect.com

REVIEW

Size-transformable nanotherapeutics for cancer therapy

Teng Ma[a], Tuyen Ba Tran[a], Ethan Lin[a], Stephanie Hunt[a], Riley Haveman[a], Kylie Castro[a], Jianqin Lu[a,b,c,d,*]

[a]*Skaggs Pharmaceutical Sciences Center, Department of Pharmacology & Toxicology, R. Ken Coit College of Pharmacy, the University of Arizona, Tucson 85721, AZ, USA*
[b]*Clinical and Translational Oncology Program, the University of Arizona Cancer Center, Tucson 85721, AZ, USA*
[c]*BIO5 Institute, the University of Arizona, Tucson 85721, AZ, USA*
[d]*Southwest Environmental Health Sciences Center, the University of Arizona, Tucson 85721, AZ, USA*

Received 28 July 2024; received in revised form 25 October 2024; accepted 4 November 2024

KEY WORDS

Drug delivery;
Size-transformation;
Self-assemble;
Smart nanomedicine;
Cancer therapy

Abstract The size of nanodrugs plays a crucial role in shaping their chemical and physical characteristics, consequently influencing their therapeutic and diagnostic interactions within biological systems. The optimal size of nanomedicines, whether small or large, offers distinct advantages in disease treatment, creating a dilemma in the selection process. Addressing this challenge, size-transformable nanodrugs have surfaced as a promising solution, as they can be tailored to entail the benefits associated with both small and large nanoparticles. In this review, various strategies are summarized for constructing size-transformable nanosystems with a focus on nanotherapeutic applications in the field of biomedicine. Particularly we highlight recent research developments in cancer therapy. This review aims to inspire researchers to further develop various toolboxes for fabricating size-transformable nanomedicines for improved intervention against diverse human diseases.

*Corresponding author.
E-mail address: lu6@arizona.edu (Jianqin Lu).

Peer review under the responsibility of Chinese Pharmaceutical Association and Institute of Materia Medica, Chinese Academy of Medical Sciences.

https://doi.org/10.1016/j.apsb.2024.11.012

1. Introduction

The rapid development of nanotechnology has enabled broad applications in biomedical research, with nanomedicine offering new opportunities for tumor treatment[1]. Compared with traditional small molecule drugs, nanomedicine boasts several advantages: 1) The nanoscale drug carrier endows it with enhanced permeability and retention (EPR) properties. This feature enables nanotherapeutics to selectively accumulate at tumor sites, thereby realizing passive targeting ability; 2) The long circulation time in the body, resulting from the size effect, prevents rapid drug elimination, enhances drug molecule stability, and circumvents degradation by the body; 3) Active targeting is achieved through carrier modification, further improving the enrichment efficiency of nanomaterials at tumor sites; 4) Integration of multiple imaging and treatment methods into a drug delivery system enables multi-modal diagnosis and treatment[2]. In 1995, The US Food and Drug Administration (FDA) granted its first approval to the anti-tumor nanotherapeutic doxorubicin liposome (Doxil) for treating Kaposi's sarcoma and multiple myeloma[3]. In 2005, the nanoparticle formulation of albumin-bound paclitaxel was approved for treating breast cancer and non-small cell lung cancer[4]. Subsequently, more nanomedicine carriers such as dendrimer macromolecules, nanogels, and polymer micelles have been developed and entered clinical settings[5]. Currently, more than 1000 nanomedicines are being tested in clinical trials[6]. Although nanodrugs have made great progress in the past ten years, they often do not perform well in clinical trials, leading to poor clinical translation. The main hurdle to the clinical conversion of nanomedicine is the low drug delivery efficiency, which is attributed to: 1) poor tumor accumulation efficiency; 2) low cellular uptake efficiency; 3) difficulty in achieving lysosomal escape in cells. A growing body of research has identified that the current level of nanodrug delivery to the target is inadequate, and the extent of accumulation and penetration at the tumor site significantly impacts intratumoral delivery[6].

There are many important factors that impact the efficiency of drug delivery, such as surface charge, coating, shape, and ligand[7]. Among these attributes, size plays a pivotal role in nanomedicine, with a crucial impact on therapeutic delivery[8,9]. The effectiveness of nanotherapeutic delivery relies on achieving both substantial accumulation and efficient penetration in tumor tissues, which are essential for reaching the site-specific treatment window and ensuring optimal treatment effectiveness[10]. Studies have indicated that cellular responses mediated by nanoparticles are contingent on size, as size can exert a substantial impact on their blood circulation duration, tumor delivery, and penetration[11,12]. Nanoparticles smaller than 5 nm can be eliminated through the kidneys, whereas those between 10 and 20 nm are quickly absorbed by the liver from the bloodstream. Particles larger than 200 nm are trapped in the splenic sinusoids or identified and removed by the reticuloendothelial system (RES). Consequently, nanoparticles within the 20−200 nm range are likely to remain in circulation for an extended period. Thus, size is a pivotal factor influencing the effectiveness of tumor-targeted drug delivery, including blood circulation, biological distribution, tumor localization and penetration, uptake by cells, and trafficking at the subcellular level[13].

Numerous studies have demonstrated a close correlation between the size of nanomedicines and their anti-tumor efficacy[14,15]. In general, the diameter of the nanomedicine is designed based on the aperture of leaky tumor blood vessels[16]. Although there may be differences due to varied tumor models, the characteristic pore size of subcutaneous tumors typically varies between 200 nm and 1.2 μm. In tumors that grow in the skull, such as brain gliomas, the size is further reduced[17]. However, nanotherapeutics face the problem that size-dependent tumor accumulation and penetration ability cannot simultaneously be optimized due to a prerequisite intricate balance. With the distinctive structure and conditions of tumor tissues, the inherent size of nanoparticles complicates efficient drug delivery. Large nanoparticles tend to remain in tumor tissues better than small nanoparticles[18−20]. On the contrary, small nanoparticles boast higher level of permeability[21,22]. To overcome this dilemma, the development of nanocarrier systems with adjustable size is of high therapeutic impact to leverage both effective retention and permeability concurrently.

After nanodrug reaches the tumor zone, substantial nanoparticles can effectively stay in the proximity of the tumor yet face obstacles in penetrating the dense matrix[23,24], while small nanoparticles can efficiently penetrate the tumors. But under the elevated interstitial fluid pressure within the tumor, small nanotherapeutics can easily be pumped back into the bloodstream[25−27], greatly undermining the delivery efficiency. Therefore, constructing a size conversion nanomedicine carrier with optimal delivery efficiency for improved anticancer efficacy represents the major challenge in nanotechnology-enabled drug delivery systems.

A variety of size-transformable nanomedicines has been reported with the aim of addressing the drawbacks mentioned above[28−32]. In this review, we summarize two types of size-transformation nanosystems for different medical applications in tumor therapy and imaging. Specifically, we cover the strategies used to switch the size from small to large and large to small. They are divided into 4 subcategories: self-assembly strategy, disassembly strategy, aggregation strategy, and degradation strategy (Scheme 1). These strategies include enzymes, pH changes, light exposure, redox reactions, temperature variations, and more, which enable leveraging their respective unique advantages in enhancing drug delivery, payload release, cellular uptake, and improving tumor imaging. Size-transformable nanodrug strategies offer significant therapeutic advantages, such as enhanced tumor targeting, improved drug accumulation and retention, deep tissue penetration, and controlled drug release. Self-assembly and aggregation strategies capitalize on increasing particle size to avoid rapid clearance and extend retention times, while disassembly and degradation strategies leverage size reduction for deeper tumor penetration and rapid clearance. However, these strategies also present challenges: complex synthesis, stability issues, potential toxicity, and difficulties in achieving precise control over size transformation and drug release. Addressing these challenges through further research is essential for optimizing these strategies for clinical applications (Table 1). Finally, the contemporary challenges and outlook of size-transformable nanomedicines are discussed.

2. Strategies from small to large

The large size of nanodrugs can extend tissue retention and attenuate exocytosis rates from cells, making them well-suited for prolonged imaging and effective treatment[33]. Furthermore, specific large nanoparticles are superior to smaller counterparts in terms of enhanced theranostics[34,35]. Numerous studies have explored strategies involving self-assembly and aggregation to concurrently enhance the accumulation and penetration of nanoparticles[36,37]. This involves employing initially small nanoparticles for deep penetration, followed by their transformation

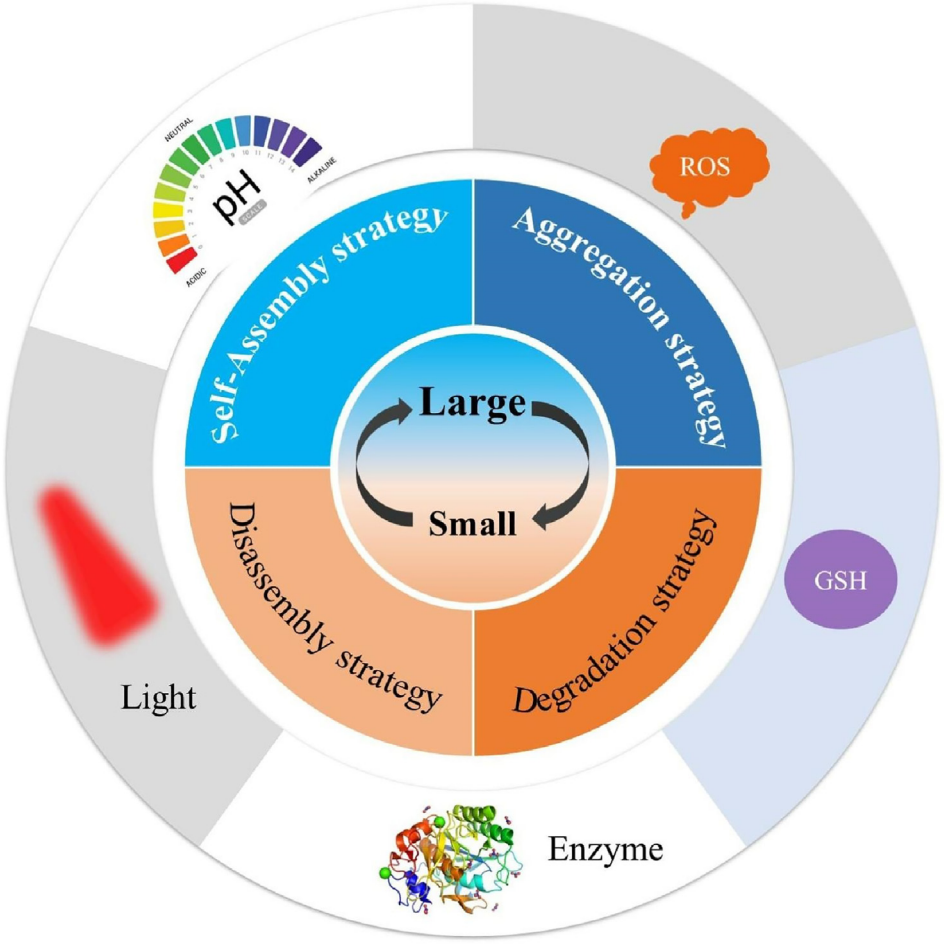

Scheme 1 Schematic illustration of the size-transformation strategy in cancer therapy.

into large nanomaterials to increase retention once deep within the tumor, triggered by specific stimuli. These stimulations are associated with internal factors such as tumor heterogeneity, categorized as hypoxia, a slightly acidic microenvironment, and the specific upregulation of enzymes. Additionally, external stimuli including light and temperature are leveraged to craft intelligent, size-aggregable nanomedicines. In response to either external or internal stimulation, the initial relatively small nanoparticles can engage in interactions through click reactions, self-assembly, electrostatic interactions, or phase transitions, ultimately leading to the formation of aggregations.

2.1. *Self-assembly strategy*

Nanodrugs can self-assemble into different kinds of assembly through hydrophobic−hydrophilic interaction[38], electrostatic interaction[39], and hydrogen bonding interactions[40], and $\pi-\pi$ stacking effects[41]. These noncovalent interactions are the main factors for spontaneous self-assembly. Hence, changing these intermolecular forces is key to designing size-transformable nanodrug. Many subfields of research are focused on tumor-specific microenvironments and external stimulation such as enzymes, pH, redox, and lasers. Once the internal or external stimulation affects the nanodrug, the initial small-sized nanodrug will transform into a large size.

2.1.1. *Enzyme-induced*

The enzyme induction strategy shows considerable potential owing to its high specificity in selecting substrates and the varied expression of enzymes across various organs/tissues[42]. Tumors, in particular, exhibit numerous specifically upregulated enzymes, including hyaluronidase (HAase), matrix metalloproteinase (MMP)[43], legumain[44], gelatinase[45], furin[46], and caspase3/7[47], among others. Enzyme-induced self-assembly capitalizes on the inherent characteristics of nanocarriers. FAP-α, an exclusive enzyme present in cancer-associated fibroblasts, functions as a prolyl oligopeptidase with specificity to cleave proline from the adjacent amino acid. As a tumor biomarker, it has been extensively used[48]. Zhao et al.[49] developed a diagnostic system with a size-switchable mechanism activated by FAP-α. This system comprises GTDTKTGPAKLVFFC (Cy) TDTG (molecule 1, Fig. 1A). Size transformation occurs through the cleavage of Gly−Pro−Ala (GPA), stimulating the release of proline and forming plentiful β-sheet fibrils. The morphological transition resulted in a 24-fold retention time increase compared to free drugs. Furthermore, the nanofibers enhanced imaging sensitivity considerably and could function as nanoprobes to expand the tumor detection limit to as tiny as 2 mm, portending an innovative way for the early diagnosis and screening of tumors.

As depicted in Fig. 1B, Hao Wang's research team[50] designed a tumor-selective cascade-activatable self-detained system (TCASS) for both tumor imaging and drug delivery. In this

Table 1 The strategies, categories, advantages, and disadvantages of size-transformation nanomedicine.

Strategy	Category	Advantage	Disadvantage
Self-assembly	Enzyme induced;	High specificity in selection, good biocompatible, and retention time;	Some enzymes in other nontarget sites, relatively long reaction time;
Disassembly	pH-induced;	High sensitivity, short reaction time;	Unstable, the uncertainty of biological distribution;
	Redox-induced;	Fast response speed;	The uncertainty of biological distribution
	Light-induced;	Precise control, non-invasive trigger, spatial selectivity;	Limited penetration depth, potential tissue damage;
Aggregation strategy	Biological orthogonal crosslinking;	High specificity, improved targeting and retention;	Complex synthesis, potential for immune response;
	Electrostatic interactions;	Simple and versatile;	Interference with biological processes;
Degradation strategy	Chemical bond break;	Multi-functionality, minimized off-target effects;	Complex design and synthesis, degradation and stability issues;
	Onion peeling strategy;	Enhanced stability, sequential release;	Potential drug loss, complex synthesis;
	Surface-binding strategy;	Simplicity in design, controlled release;	Limited drug loading capacity;

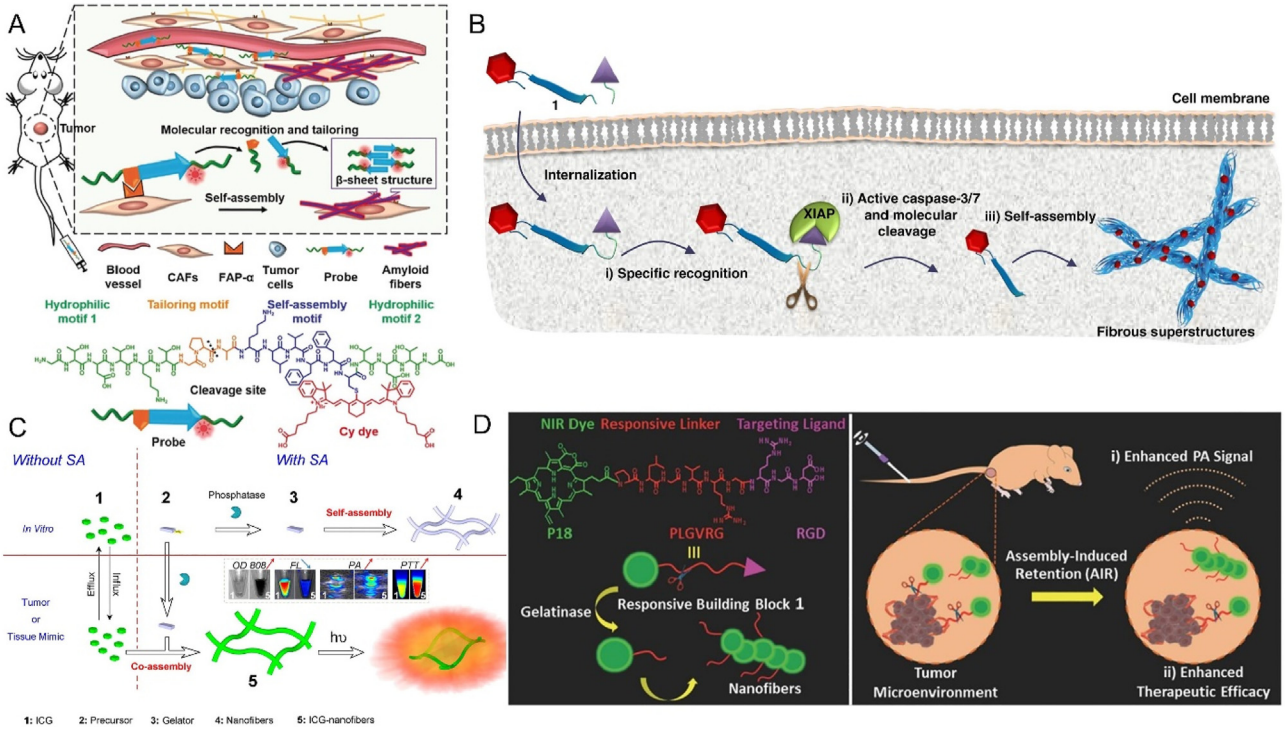

Figure 1 (A) Schematic of *in situ* self-assembly of nanofibers guided by cancer-associated fibroblasts (CAFs) for heightened tumor imaging, accompanied by the chemical structure of the probe featuring four motifs. Reprinted with permission from Ref. 49. Copyright © 2019 Wiley-VCH Verlag GmbH & Co. KGaA, Weinheim. (B) The process entails the specific identification, molecular cleavage, and on-site self-assembly of molecule **1**. Initially, the X-linked inhibitor of apoptosis protein (XIAP) specifically recognizes molecule **1**. Subsequently, the activated caspase-3/7, triggered by the identification process, cleaves the molecules. Following this cleavage, the molecules undergo rapid self-assembly *in situ*, forming fibrous β-sheet superstructures. Ultimately, these nanostructures made of β-sheets are crucial in enhancing the accumulation and retention of functional molecules within the tumor tissue. Reprinted with the permission from Ref. 50. Copyright © 2019 Springer Nature. (C) The Schematic of the enzyme-triggered supramolecular coassembly of compounds **1** and **2**. Reprinted with the permission from Ref. 52. Copyright © 2015 American Chemical Society. (D) Illustration depicting the structural arrangement of compound **1** and its adaptive self-assembly into nanofibers within tumor sites, highlighting the amplification by stimulated emission of radiation (AIR) effect. Reprinted with the permission from Ref. 45. Copyright © 2015 Wiley-VCH Verlag GmbH & Co. KGaA, Weinheim.

system, small molecule peptides are engineered for the specific recognition and targeting of X-linked inhibitors of apoptosis protein (XIAP), a protein significantly elevated in tumor cells. The interaction with XIAP triggers caspase-3 activation, enabling molecular shearing and self-assembly into nanofiber structures that enhance the accumulation and retention in tumor sites. Furthermore, TCASS exhibited metabolism similar to small molecules, allowing for rapid clearance from the kidneys and liver and mitigating systemic toxicity. Responsive to enzymatic stimuli, TCASS improves the therapeutic effectiveness of conventional chemotherapy drugs while abrogating their adverse effects. By coupling with contrast agents, the specificity and sensitivity of imaging agents are markedly improved, demonstrating excellent imaging performance in a human bladder cancer model. This study provides a novel tumor targeting mechanism, accelerating the application of nanodrugs and opening new avenues for basic research and clinical translation of nanodrugs.

Alkaline phosphatase (ALP), an enzyme overexpressed in stem cells and certain cancer cells that rapidly converts ATP into adenosine, has been identified as a cancer biomarker for over half a century ago[51]. Huang et al.[52] established a co-assembly strategy instigated by endogenous phosphatase, leading to the formation of tumor-specific nanofibers incorporating indocyanine green (ICG) for cancer therapy. Utilizing coordinated intermolecular interactions, the size-transformable nanofiber brought about significant alterations in the near-infrared absorbance of ICG, which in turn, enhanced its crucial photoacoustic and photothermal performance. The enzyme-guided co-assembly process and its therapeutic capabilities were successfully demonstrated *in vitro*, live cells, tissue-mimicking models, and *in vivo* (Fig. 1C). 4 h post intravenous injection, the ICG uptaken by tumor notably elevated to 15.05 ± 3.78% ID/g, a 25-fold increase compared to free ICG. This yielded a high tumor-to-normal tissue (*T*/*N*) ratio (>15). Finally, this nanosystem effectively eliminated tumors, demonstrating high-precision treatment.

MMP-2 (matrix metalloproteinase-2) and MMP-9 (matrix metalloproteinase-9) are members of the matrix metalloproteinase family[53]. Their roles in cancer progression involve enzymatically degrading the extracellular matrix (ECM), detaching cancer cells from the primary tumor. This process enables the migration of cancer cells to distant sites, where they form metastatic lesions[54]. These enzymes are frequently overexpressed in the tumor microenvironment and selectively cleave peptide substrates with the sequence of PLGVRG. Zhang et al.[45] devised a peptide sequence, P18-PLGVRGRGD, capable of self-assembling into nanofibers within the tumor. This design amplified both photoacoustic (PA) signal and therapeutic effects (Fig. 1D). Transmission electron microscopy (TEM) validated nanofibers formation in P18-PLGVRGRGD buffer solution when incubated with MMP-2/9. The Purpurin 18 molecules overlapping and $\pi-\pi$ stacking interactions between the molecules gave rise to nanofibers with a width of 3.8 nm. Leveraging a small hydrophilic RGD peptide ligand facilitated the targeted delivery of nanofibers to $\alpha v\beta 3$ integrin on the cancer cell membrane. MMP cleavage of the PLGVRG linker enhanced the molecule's hydrophobicity, reducing steric hindrance and facilitating self-assembly into nanofibers with the near-infrared dye P18 in the tumor. Ultimately, as the anhydride groups on P18 underwent gradual hydrolysis, the hydrophilicity of the gel-like molecules increased, leading to nanofibers degradation and subsequent clearance of P18 from the solid tumor. Following injection of P18-PLGVRGRGD, within 10 h, the amount of P18 at the tumor site was almost 7-fold greater than the control group. Concurrently, an elevated photoacoustic signal was observed with tumor inhibition. This suggests that assembly-induced retention can amplify the tumor-targeted imaging capabilities of P18 and subsequently enhance the effectiveness of photothermal therapy (PTT).

2.1.2. *pH-induced*

Rapidly proliferating cancer cells display increased glycolytic activity, leading to an acidic extracellular pH (pHe) in tumors compared to normal tissue[55]. The pHe of tumor tissue is approximately 6.8−7.2, whereas normal tissue has a pHe of around 7.4[56]. Within tumor cells, the pH levels in the nucleus (5.0−5.5) and lysosomes (4.5−5.0) can be further reduced[57]. Recently, diverse strategies have been identified for creating pH-responsive nanocarrier systems with size transformation potential. In contrast to the aggregation induced by enzymes, pH-induced reactions provide swift responsiveness and heightened sensitivity. Histidine can be protonated at pH 6.5, an acidic condition frequently employed for constructing pH-responsive nanocarriers[58]. As shown in Fig. 2A, Yang et al.[59] developed an in-situ peptide-based self-assembling nest-like host for non-invasive implantation in tumor regions for homing therapy of drugs. The peptide was comprised of four segments: (1) a hydrophobic aromatic bispyrene module, (2) a hydrogen-bonding peptide KLVFF module derived from Aβ, selected as the peptide scaffold for the formation of β-folded fibers with enclosed hydrophobic domains, (3) polyethylene glycol as a hydrophilic chain, and (4) a pH-sensitive peptide sequence. Initially, in a phosphate buffer solution BP-KLVFF-His6-PEG self-assembled into nanoparticles, manifesting green fluorescence due to bispyrene aggregation. The nanoparticles were administered intravenously to mice with tumors, accumulated at the tumor site *via* the EPR effect, and then transformed into nanofibers attributed to changes in hydrophilic/lipophilic balance triggered by the acidic tumor microenvironment, thus forming a nest-like host with a β-folded structure. The host enveloped the tumor area, extending a retention of up to 96 h, enabling the binding and concentration of guest molecules, including doxorubicin (DOX), Nile Red (NR), and ICG that were embedded into the hydrophobic regions of the β-folded nanofibers. 96-h post intravenous injection, the tumor exhibited significant accumulation of NR, with a fluorescence intensity 7.5-fold greater than the free NR group. Concurrently, ICG and DOX molecules were concentrated in tumor sites, facilitating effective chemotherapy and photothermal therapy, respectively. This innovative approach laid the foundation for creating tumor-specific hosts that can accumulate therapeutic drugs under pathological conditions, prolonging retention and sustained release.

Han et al.[60] developed a hybrid peptide responsive to extracellular tumor acidity, designed to undergo geometric shape transformation to enhance tumor internalization and improve photodynamic therapy (Fig. 2B). Under physiological conditions, this hybrid peptide self-assembles into nanoparticles. However, within the acidic tumor microenvironment, the acid-sensitive group 2,3-dimethylmaleic anhydride detaches from the hybrid peptide, and can detach, resulting in ion-complementary restoration among hybrid peptides and the formation of rod-shaped nanoparticles. Their results showed that the pH-triggered size transformation of the hybrid peptide accelerated its internalization into tumor cells, prolonged tumor retention, enhanced photodynamic therapy, and reduced side effects. These findings support the effectiveness of the size transformation strategy based on the acidity of the tumor microenvironment in improving therapeutic delivery efficiency.

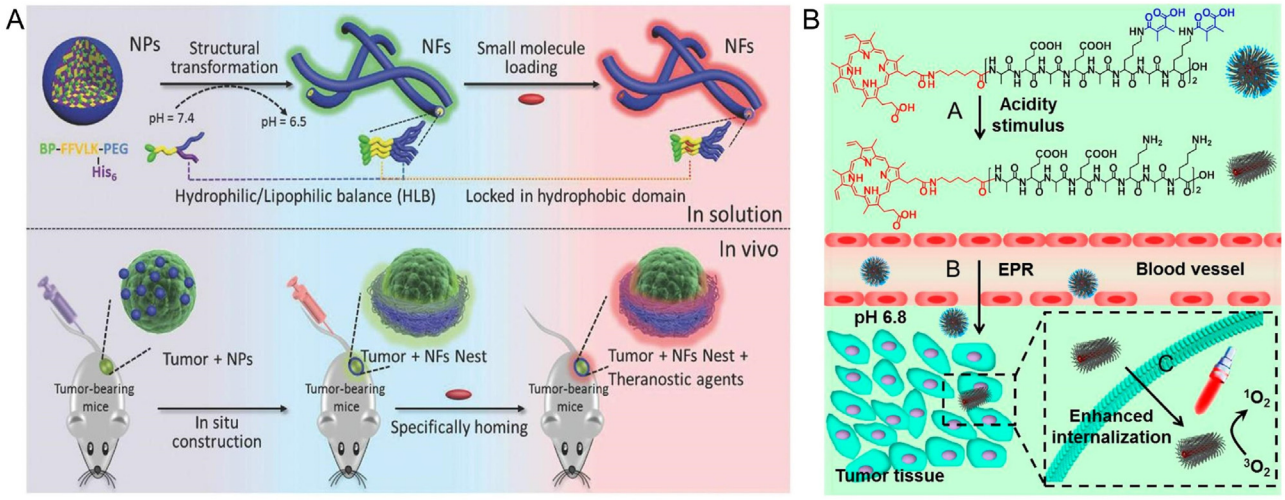

Figure 2 (A) Illustration depicting the composition of the molecule, the mechanism behind shape transformation, and the strategy for drug homing. Reprinted with the permission from Ref. 59. Copyright © 2017 Wiley-VCH Verlag GmbH & Co. KGaA, Weinheim. (B) Schematic depiction of an acidity-triggered size transformation leading to enhanced photodynamic therapy (PDT). Reprinted with the permission from Ref. 60. Copyright © 2017 American Chemical Society.

2.1.3. *Redox-induced*

The heightened proliferation of aggressive tumors leads to elevated levels of oxidative stress in both tumor tissues and cells, manifested by increased levels of reactive oxygen species (ROS)[61]. In response to oxidative stress, there is a concomitant increase in the oxidative-reductive environment within tumors[62]. For instance, the glutathione (GSH) level inside tumor cells rises to enhance antioxidant capacity, combat oxidative stress, and regulate cell differentiation, proliferation, and apoptosis[63]. Research indicated that GSH concentrations in tumor regions, especially intracellularly, can reach ∼2−10 mmol/L, whereas in normal tissues, it ranges from ∼2 to 20 μmol/L[64,65]. Disulfide bonds are chemical groups that can be reduced to thiol groups by GSH response making them valuable in drug delivery systems that exploit redox environments[66]. Guo et al.[67] developed a PEG-dithiothreitol (TGA)-NapFFKY delivery system responsive to redox conditions. The disulfide bonds are cleaved in the presence of a high concentration of glutathione, decreasing hydrophilicity. Consequently, hydrophobic interactions and hydrogen bonding are enhanced, promoting the formation of β-folds and facilitating the transition to nanofibers. Compared to free DOX, the DOX-laden nanotherapeutic exhibited decreased systemic toxicity, with a lower half-maximal inhibitory concentration and an elevated apoptosis rate in tumor cells (2.4-fold higher), indicating a synergistic effect of self-assembling nanofibers with chemotherapy. Moreover, this nanosystem with shape-shifting capabilities enabled efficient systemic administration of DOX by overcoming the poor solubility encountered during intravenous delivery of nanofibers, resulting in increased effective drug concentration within tumor cells (Fig. 3A).

In the majority of cancer cells, there is an overproduction of ROS in the vicinity of mitochondria[68−71]. Drug delivery systems featuring ROS-responsive bonds have been extensively investigated[72] and can achieve oxidative stress-induced size-transformation. ROS triggers the size transformation of Polymer-Peptide Conjugates (PPCs), which interact with mitochondria and demonstrate high efficacy in tumor treatment[73]. PPCs consist of (1) a ROS-cleavable sulfone-linked polyethylene glycol (PEG) coupled to a β-sheet forming peptide KLVFF, (2) a cytotoxic peptide KLAK specifically targeting mitochondria, and (3) a PEG main chain. PPCs nanoparticles can enter cells and target mitochondria. Given the excess ROS production around mitochondria in cancer cells, the sulfone linker can be cleaved, leading to the shape transition of nanoparticles to nanofibers (Fig. 3B). The exposed nanofibers at the KLAK positions heightened interactions with mitochondria involving multiple binding sites and cooperative effects, resulting in targeted cytotoxicity against cancer cells and effective tumor suppression *in vivo*.

2.1.4. *Light-induced*

The photo-induced approach offers advantages such as non-invasiveness, remote operation, and simplicity[74]. Recently, photothermal response strategies have garnered considerable attention owing to their precision, non-invasiveness, environmental friendliness, remote control, and convenience[75]. Commonly, photosensitive therapy materials incorporate photo-responsive groups like nitrobenzene, diazo, or diazenyl groups, and acrylic groups[76]. Regarding light-induced polymerization strategies, photosensitive polymers integrate photoreactive groups such as azobenzene, spirogyran, triphenylmethane, or cinnamyl. These groups exhibited reversible structural changes upon exposure to UV−Vis light[77−80]. Cheng et al.[81] reported light unstable gold nanoparticles (AuNPs) modified with dinitroimidazole (DA) at the end of the ligand PEG_{5000} (MW = 5000), can covalently crosslink under 405 nm laser irradiation. As illustrated in Fig. 4A, upon 405 nm laser excitation, the surface dinitroimidazole on particles first converted to a carbene that subsequently formed covalent bonds through C/H, C/C, O/H, and X/H (X = heteroatom) on the ligands of adjacent AuNPs, yielding aggregation of AuNPs. The robust coupling among the aggregated AuNPs *in vivo* caused an effective shift of the surface plasmon resonance peak of 20.5 nm AuNPs toward the near-infrared region. This enabled the use of small AuNPs for not only improved photoacoustic imaging but also efficient photothermal therapy of malignant tumors.

As shown in Fig. 4B, Liu et al.[82] developed a nano-drug, IP@NPs@M, coated with a thin film, which boasted

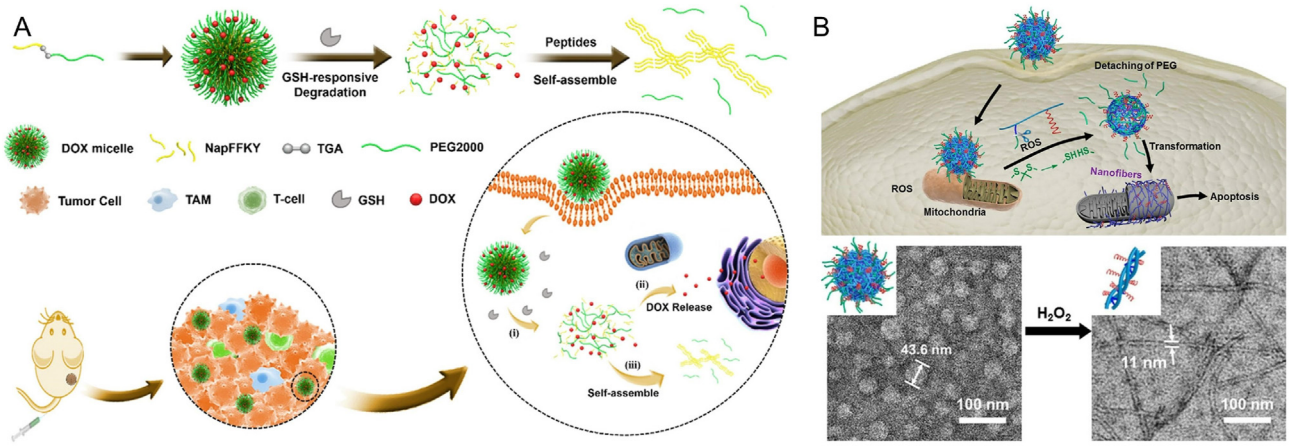

Figure 3 (A) Schematic representation illustrating the intracellular restructuring of a GSH-responsive drug delivery system on transitioning from micelles into nanofibers. Reprinted with the permission from Ref. 67. Copyright © 2020 American Chemical Society. (B) Schematic of ROS-induced size-transformation with shape transition from nanospheres to nanofiber. Reprinted with the permission from Ref. 73. Copyright © 2019 American Chemical Society.

morphological transformation and light-responsive properties. Under laser irradiation, the photosensitizer can produce ROS, leading to a change in the hydrophilicity of bilirubin. This change caused the nanoparticles to transition from a spherical to a fibrous shape, significantly improving drug retention at the tumor site. Due to the morphological and size transformation, the combination therapy of PDT, chemotherapy, and immunotherapy elicited remarkable efficacy by markedly suppressing tumor growth and reducing metastasis. Ma et al.[83] reported a novel nano-drug, DEVD-DLPA@C3 NPs for caspase-3 responsive tumor treatment. This nanosystem was composed of a dual amphiphilic peptide (DEVD-DLPA) with a diacetylene moiety and a mitochondria-targeting photosensitizer (C3) (Fig. 4C). DEVD-DLPA@C3 NPs increased drug delivery efficiency by actively

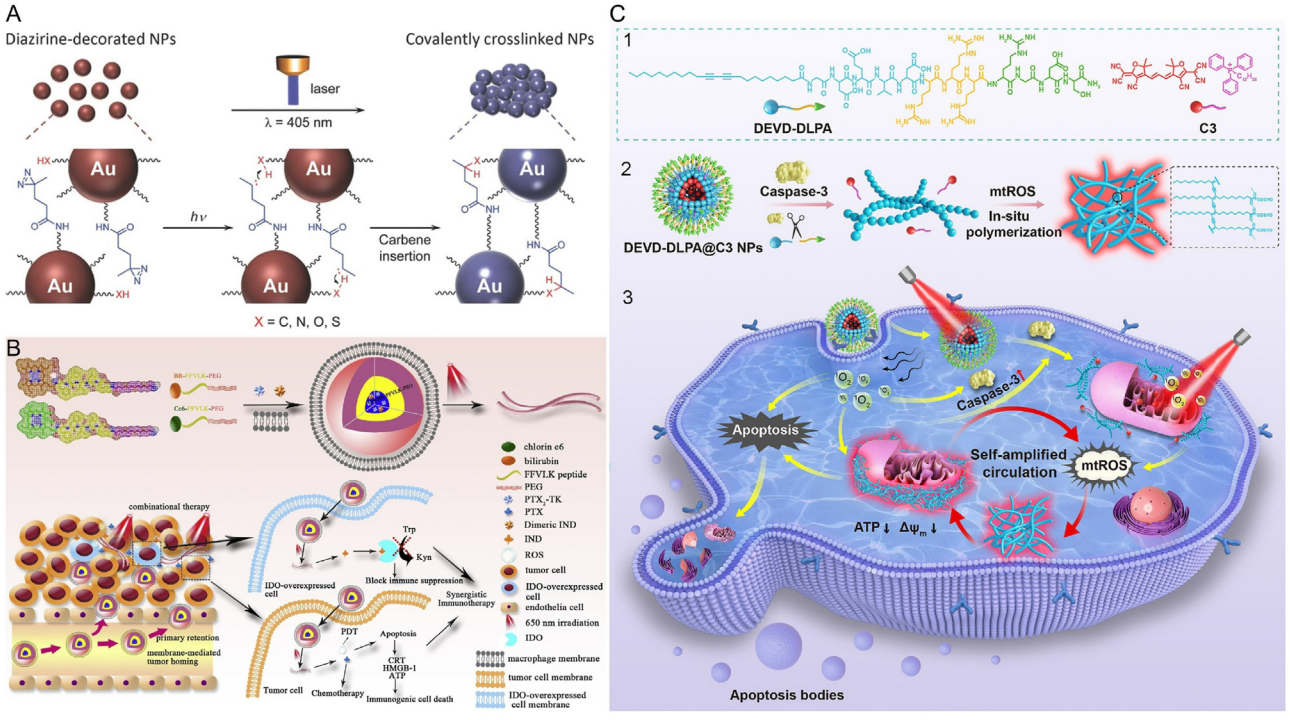

Figure 4 (A) Illustration depicting the light-triggered assembly of dendritic gold nanoparticles (dAuNPs). Reprinted with the permission from Ref. 81. Copyright © 2017 Wiley-VCH Verlag GmbH & Co. KGaA, Weinheim. (B) Schematic illustration depicting the change of IP@NPs@M nanoparticles from spherical micelles to nanofibers under 650 nm laser irradiation. Reprinted with the permission from Ref. 82. Copyright © 2020 Elsevier. (C) 1. The compositions of DEVD-DLPA and C3. 2. Illustration depicting the morphological transition from nanoparticles to nanofibers. 3. Schematic illustration portraying photodynamic therapy (PDT) triggered *in situ* intracellular polymerization, resulting in mitochondrial ROS burst and self-amplified circulation of tumor therapy. Reprinted with the permission from Ref. 83. Copyright © 2022 Wiley-VCH Verlag GmbH & Co. KGaA, Weinheim.

targeting tumor cells through an affinity interaction with the RGDS peptide and integrins. Under laser irradiation, the generated ROS initiated the apoptotic process, demonstrative by over-expression of caspase-3 and the release of photosensitizer. Upon a second laser irradiation, free photosensitizer on mitochondrial generated singlet oxygen, disrupting the mitochondria and causing a mitochondria ROS (mtROS) burst. Significantly, the ROS produced *via* photodynamic action and the mtROS burst cleaved DEVD-DLPA by caspase-3, leading to the transformation of spherical NPs into elongated nanofibers through efficient *in-situ* polymerization. This transformation resulted in a more severe mtROS burst, thereby maximizing the effectiveness of the nanomaterial.

2.2. *Aggregation strategy*

In addition, some research groups have designed smart nanoparticles that aggregate in response to both external and internal stimuli, including pH, light, and enzymes. When subjected to these stimuli, initially small nanoparticles aggregated through interactions such as click reactions, electrostatic interactions, or phase transitions, resulting in the formation of larger nanoparticles.

2.2.1. *Biological orthogonal crosslinking*

Due to the simplicity and speed, click reactions are often employed in enzyme-induced size transformations. Typically, functional groups capable of undergoing click reactions, such as azides and alkynes[84], thiols and maleimides[85], and 1,2-dithiolanes and cyanides[86,87], are decorated on the surface of nanoparticles. Upon exposure and interaction of these chemical groups following enzyme cleavage reactions, rapid aggregation occurs, yielding the formation of larger nanoparticles. As shown in Fig. 5A, Ruan et al.[88] proposed a strategy for enhancing the retention of chemo drugs for brain tumors using an asparagine endopeptidase-triggered gold nanoparticle aggregation platform. This platform consists of gold nanoparticles modified with Ala-Ala-AsnCys-Lys (AuNPs-AK) and gold nanoparticles modified with 2-cyanobenzothiazole (AuNPs-CABT). AuNPs-AK is hydrolyzed by asparagine endopeptidase in glioma cells, exposing the 1,2-dithiolane on the nanoparticle surface. Subsequently, it engaged in a click cycloaddition reaction with neighboring cyanide groups on AuNPs-CABT, leading to the aggregation of AuNPs. This approach improved the retention of gold nanoparticles, attributed to hindering nanoparticle efflux into the bloodstream. Efficiency in treating gliomas is enhanced when doxorubicin (DOX) is attached to AuNPs-A&C through a pH-sensitive linker. Compared to the saline group, DOX-conjugated AuNPs-A&C increased the average survival time by 288% in mice, as assessed with multi-spectral optoacoustic tomography for effective *in vivo* imaging. This study offered a strategy to enhance nanoparticle accumulation in tumors and improve therapeutic outcomes for tumors.

3. Electrostatic interactions

Surface charge is commonly employed for nanoparticle stabilization, and nanoparticles with a positive charge can form cross-links with those carrying a negative charge[89–91]. Nam et al.[92] produced amine-functionalized AuNPs with a positive charge and modified them with a pH-sensitive citramide group to invert the surface charge of the AuNPs. The citramide moiety remains

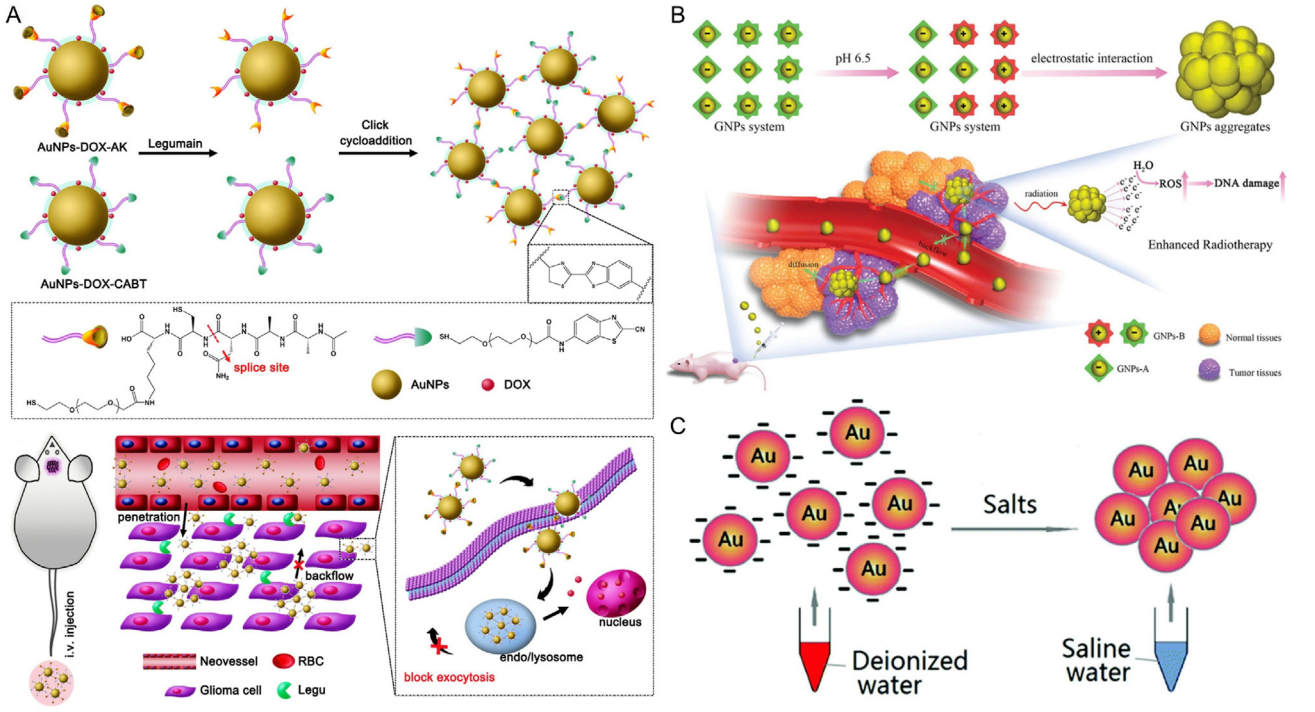

Figure 5 (A) Schematic illustration represents the legumain-induced aggregation and composition of AuNPs-DOX-A&C. Reprinted with the permission from Ref. 88. Copyright © 2016 American Chemical Society. (B) Diagram illustrating the behavior of the AuNPs system *in vivo* after intravenous injection, showcasing enhanced tumor retention and increased radiotherapy (RT). Reprinted with the permission from Ref. 83. Copyright © 2019 Wiley-VCH Verlag GmbH & Co. KGaA, Weinheim. (C) Schematic of the salt-induced aggregation of AuNPs that bear a negative charge with citrate. Reprinted with the permission from Ref. 95. Copyright © 2016 The Royal Society of Chemistry.

stable under neutral or alkaline conditions but undergoes hydrolysis to citric acid at pH values below 7.0. Consequently, when the terminal functional group transitioned from a carboxylic acid anion to a protonated amine, the surface molecules acquired a positive charge. Subsequently, the negatively charged, unhydrolyzed AuNPs can crosslink with the positively charged AuNPs. In addition, a strategy based on the acid-triggered small AuNPs was proposed by Zhang et al.[93] for the aggregation of AuNPs within tumors. The resultant AuNPs aggregates served as radiation sensitizers in both *in vivo* and *in vitro* applications (Fig. 5B). The AuNPs improved the accumulation and retention of AuNPs in cells and tumor sites, resulting in a notable enhancement in the radiation sensitization effect for tumor radiotherapy. This was substantiated by studies using DNA breakage and comet assays, where the sensitivity enhancement ratio (SER) for the AuNPs system was much higher (1.730) compared to the single AuNPs system (1.16) in MCF-7 cancer cells. *In vivo*, anti-tumor investigations also demonstrated that the AuNPs system bolstered the sensitivity of MCF-7 tumor transplants to radiotherapy. Additionally, the aggregation of AuNPs enhanced the signal of photoacoustic imaging *in vivo* of small AuNPs. This research provided novel strategies and insights for developing nanoparticle aggregates to boost the efficiency of radiation sensitivity in nanosystems for cancer radiotherapy.

4. Screening electrostatic effect-induced aggregation

Electrostatic repulsion plays a crucial role in the colloidal stability of nanoparticles, inhibiting their aggregation[94]. Sun et al.[95] developed a method for inducing the aggregation of AuNPs through salt in biological environments, creating an effective and biocompatible near-infrared photothermal transducer for cancer photothermal therapy (PTT) and PA/PT imaging (Fig. 5C). The *in situ* formation of AuNPs depot through salt-induced aggregation exhibited strong near-infrared absorption due to plasmon coupling between adjacent AuNPs, achieving a remarkably high photothermal conversion efficiency of 52%, enabling the photothermal elimination of cancer cells. Interestingly, the *in situ* aggregated AuNPs depot in the tumor can simultaneously perform tumor PA/PT imaging and PTT. These findings offered a straightforward and effective approach to developing a smart, biocompatible, and efficient near-infrared photothermal sensor for PT/PA imaging and PTT.

5. Strategies from large to small

As discussed earlier, the relationship between nanoparticle size and intratumoral behavior is impacted by elevated interstitial fluid pressure and the dense matrix commonly found in solid tumors[24,25]. These factors hinder thorough penetration and uniform distribution of nanoparticles within the tumor[96,97]. Hence, reducing nanoparticle size is essential to enhance penetration. Furthermore, the size of nuclear pores (reported to be ~10 nm, expanded to as much as 39 nm)[98] restricts the size of nanoparticles that can target the nucleus. Shrunken nanoparticles not only maintain a compact size for improved penetration but also influence various other characteristics, including drug release, secondary distribution, and rapid renal clearance[99–101]. Thus far, a diverse array of nanoparticles has been explored using two strategies: reassembly and degradation. These strategies are enabled by endogenous pH, elevated enzyme levels[102], redox reactions, and exogenous physical-chemical stimulation.

5.1. *Reassembly strategy*

5.1.1. *pH-induced*

Block copolymers (BCPs) serve as a highly versatile platform for designing smart nanosystems[103], and their applications in cancer therapy have made significant progress[104,105]. There is ongoing interest in investigating the morphology and responsiveness of BCP-based nanosystems to fully utilize their therapeutic potential. As shown in Fig. 6A, Cao et al.[106] constructed a biodegradable block copolymer assembly with pH-responsive behavior, which changed in size to form smaller, highly penetrable cationic nanocarriers under low pH conditions. This was achieved by modifying imidazole domains in flexible poly(carbonate) to a pK_a of ~6.5, enabling pH-induced changes in BCP amphiphilicity and charge reversal under tumor microenvironment pH conditions. The dynamic alterations in size and adjustable surface charge of this biodegradable nanocarrier offered optimal physicochemical characteristics for accomplishing targeted drug delivery and facilitating deep penetration at tumor sites.

2,3-Dimethylmaleic anhydride (DMA) undergoes a reaction with different amines to produce acidic amines. These acidic amines then undergo further reactions and decomposition into an amine and DMA under weak acidic conditions[107]. As shown in Fig. 6B, Li et al.[108] developed a PCL-CDM-PAMAM/Pt formulation that switched size from 100 to 5 nm in the acidic pH environment within tumors. This structural change greatly promoted tumor penetration and cellular uptake of the therapeutic drug. The internalized prodrugs further released cisplatin to kill cancer cells intracellularly. The *in vivo* antitumor efficacy of this nanodrug system was confirmed in low-permeability pancreatic cancer, metastatic tumors, and drug-resistant tumors, highlighting its adaptability and wide applicability in cancer therapy. DMA, in addition to its direct decomposition to decrease size, displays an additional feature of charge reversal for the creation of smaller nanoparticles (as shown in Fig. 6C)[109]. Sun et al.[102] constructed a core-satellite nanostructure system, denoted as MSN-Fe-CAuNC (MFA), comprising mesoporous silica nanoparticles (MSN) and cysteamine-functionalized gold nanoclusters (CAuNC). Iron ions (Fe^{2+}) were employed as bridging ions coordinated with amino groups. The ionic ligands are sensitive to acidic pH, allowing the core-satellite structure to dissociate in the tumor microenvironment, leading to volume reduction. Achieving substantial size reduction and altering the charge are crucial for facilitating penetration and uptake by cells within tumors. Although pH-triggered methods exhibit sensitivity and specificity due to the prevailing acidic conditions and presence of proton, acidic and hypoxic areas are frequently located distantly from blood vessels. This poses a notable challenge for pH-induced size reduction strategies[110]. Ma and colleagues[111] have developed a multifunctional dual-component peptide nanomedicine capable of size-shifting in response to the changing forces of intermolecular interactions within the acidic conditions of the tumor microenvironment. They utilized two peptides, C12-K(Dye)EEEGRGDS (PA1) with a negative charge and CKKK-SS-DOX (PA2) with a positive charge, which self-assembled through electrostatic interactions and hydrophobic forces (Fig. 6D). These self-assembled dual-component nanoparticles (PP NPs) possessed an appropriate size and near-neutral charge, prolonging circulation time and stability *in vivo*. Upon reaching the tumor tissue, PA1 and PA2 responded to the tumor microenvironment pH and laser irradiation, leading to their reassembly into smaller nanoparticles. *In vitro* and *in vivo* investigations using near-infrared fluorescence

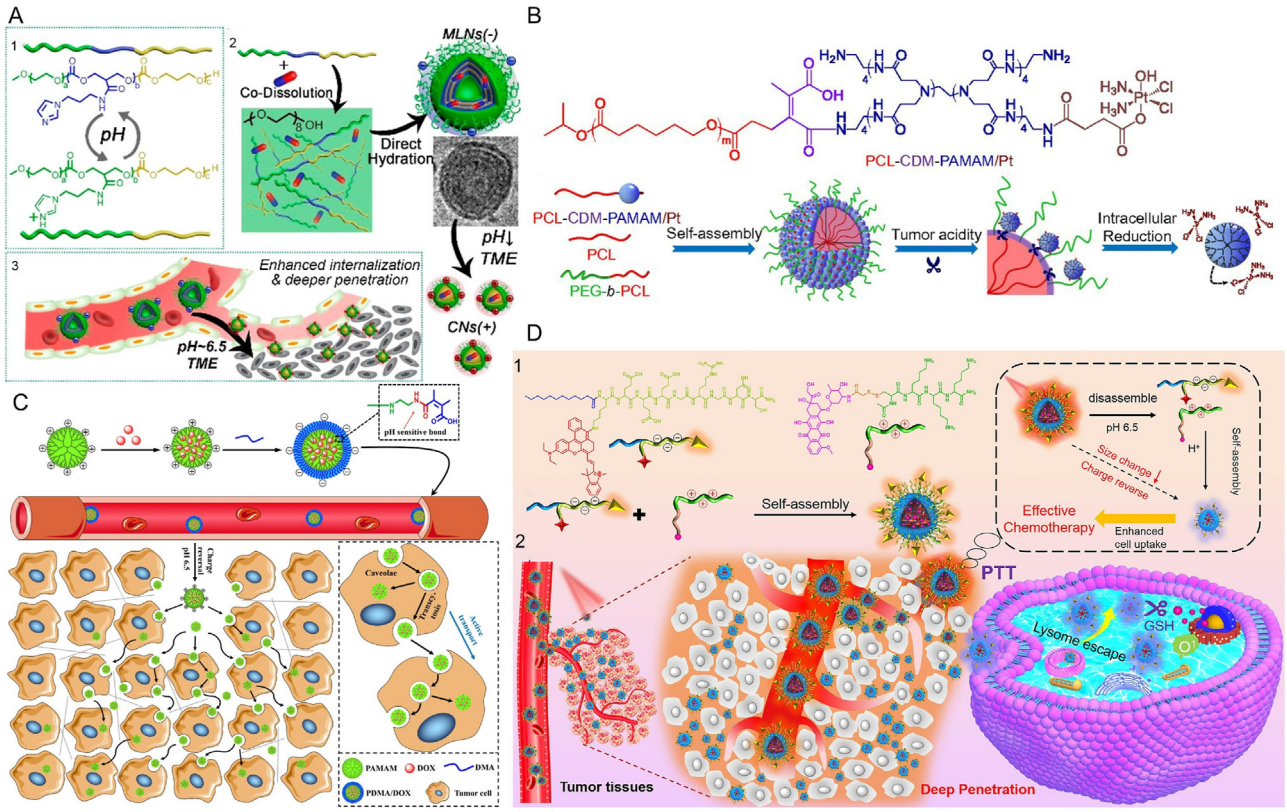

Figure 6 (A) 1. The chemical structure of PEG-TMCI-TMC terpolymers and the protonation of imidazole moieties induced chemical transformation at low pH. 2. Drug-loaded multilamellar nanovectors (MLNs) are generated through direct hydration and undergo structural reconfiguration at low pH, resulting in their transformation into cationic nanovectors (CNs). 3. The anticipated mode of action of MLNs *in vivo* involves the localized pH reduction in the tumor microenvironment, thereby enhancing the internalization of CNs and improving tumor penetration. Reprinted with the permission from Ref. 106. Copyright © 2018 American Chemical Society. (B) The chemical structure of PCL-CDM-PAMAM/Pt and the process of self-assembly and structural changes of iCluster/Pt in tumor responses. Reprinted with the permission from Ref. 108. Copyright © 2016 National Academy of Sciences. (C) Schematic representation of the structure of DMA-based nanomicelles and the illustration of pH-responsive size shrinkage. Reprinted with the permission from Ref. 109. Copyright © 2020 American Chemical Society. (D) 1. Diagram depicting the creation of multifunctional two-component nanoparticles (PP NPs) facilitated by electrostatic interactions between PA1 and PA2. 2. Illustration of the tumor-targeting and size-transformable characteristics of PP NPs for enhanced tumor penetration and efficient photochemical combined anticancer therapy. Reprinted with the permission from Ref. 111. Copyright © 2022 Wiley-VCH Verlag GmbH & Co. KGaA, Weinheim.

imaging showed that the transformed smaller nanoparticles were readily taken up by tumor cells and penetrated the tumor effectively. Crucially, the disassembled PP NPs demonstrated phototherapeutic effects comparable to those of intact PP NPs and exhibited superior chemotherapeutic efficacy in the deeper regions of tumors. PP NPs integrated fluorescence imaging, tumor targeting, tumor penetration, and phototherapy, leading to promising *in vivo* anti-tumor effects.

5.1.2. Redox-induced

Given the crucial role of GSH levels in both cytoplasm and tumor tissues, their influence is also evident in approaches that trigger size reduction[112,113]. As shown in Fig. 7A, Guo and colleagues[114] designed a nanomicelle structure using polyethylene glycol-*co*-polylactic acid (PEG-PLA) and polyethyleneimine modified with 2,3-dimethylmaleic anhydride (PEI-DMA). These components were linked by disulfide bonds, resulting in the formation of PEG-PLA-S-S-PEI-DMA (PELESS-DA). Upon reacting with the high concentration of GSH inside cells, the PEI shell detached. Moreover, the significant decrease in size enabled the shrunken nanoparticles to enter the cell nucleus, subsequently facilitating the release of the DOX. Nuclear delivery ensured the drugs efficacy against its target, preventing exclusion from the cells by drug efflux proteins, a critical aspect in nuclear-targeted chemotherapy drug delivery. Similarly, Wang et al.[115] designed and synthesized PSPD/P123-Dex hybrid nanomicelles (Fig. 7B). Under conditions of high intracellular GSH concentration, the nanomicelles with a size of 120 nm significantly shrank to ∼30 nm for P123-Dex. Owing to its ideal small size and the aid of dexamethasone, P123-Dex facilitated the transport of encapsulated DOX into the cell nucleus, leading to considerable cytotoxic effects.

6. Light-induced

The optical and photothermal properties of photosensitizers can be harnessed to design nanoscale drug carriers with size-transforming capabilities[116]. As shown in Fig. 7C, Chen et al.[117] integrated the benefits of photo-responsiveness and shape transformation in the design of a nanodrug utilizing the BF2-azadipyrromethene (aza-BODIPY) dye. Because of the favorable photothermal property of

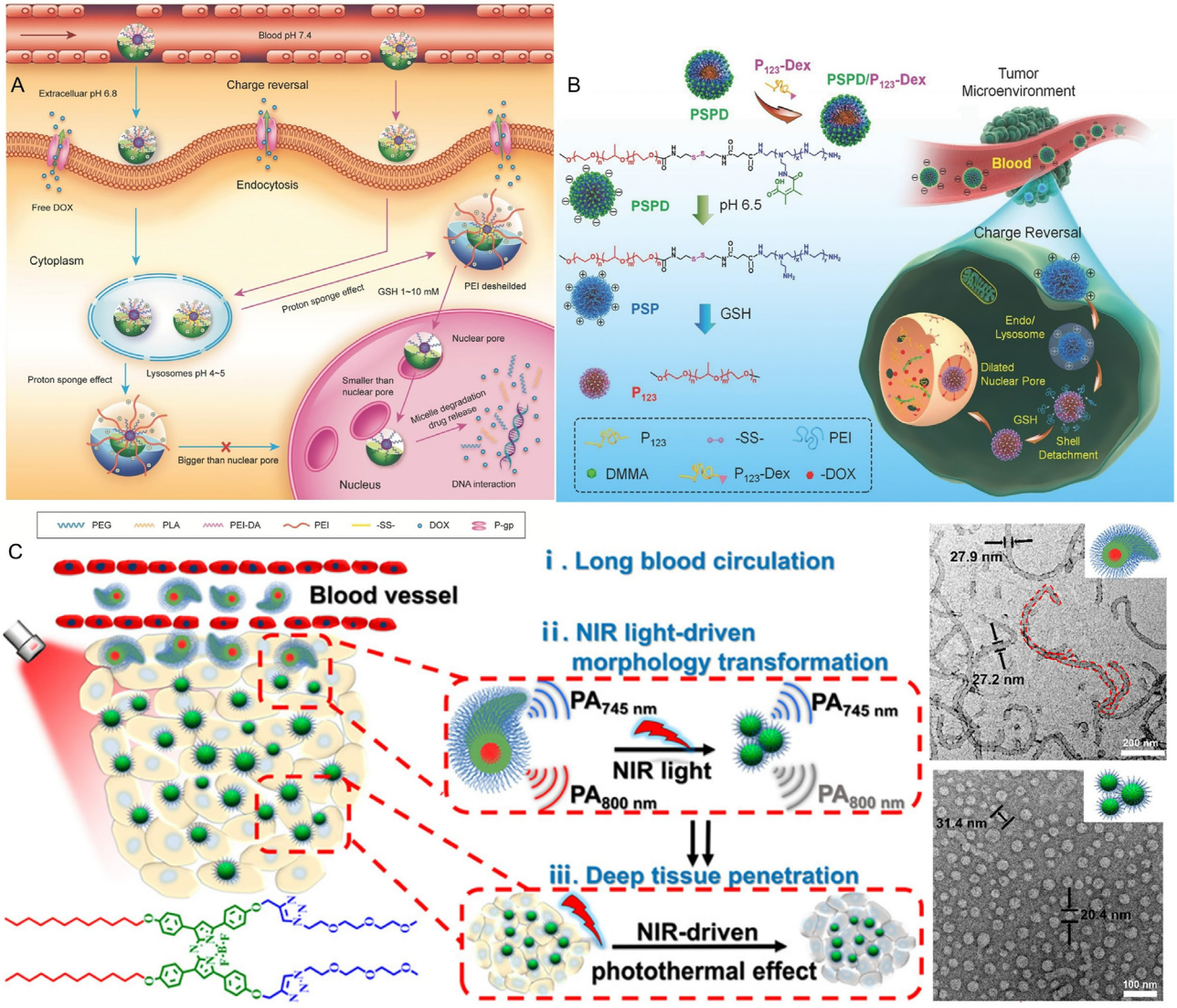

Figure 7 (A) Schematic illustration of the nuclear entry mechanism of size-shrinking polymer micelles (PELESS-DA) overcoming multidrug resistance (MDR). Reprinted with the permission from Ref. 114. Copyright © 2015 Wiley-VCH Verlag GmbH & Co. KGaA, Weinheim. (B) Schematic illustration of the hybrid micelle PSPD/P123-Dex-mediated synergistic size strategy for anticancer drug delivery. Reprinted with the permission from Ref. 115. Copyright © 2017 Wiley-VCH Verlag GmbH & Co. KGaA, Weinheim. (C) 1. Schematic illustration of amphiphilic Aza-BODIPY-1 transforming from nanofibers to micelles under near-infrared light irradiation. 2. Long circulation of nanofibers in the bloodstream and deep penetration of spherical micelles into tumors. Reprinted with the permission from Ref. 117. Copyright © 2020 American Chemical Society.

aza-BODIPY nanoclusters, the thermodynamically stable fibrillar aggregates can undergo a transformation into a metastable spherical micelle. Elevating the temperature extended the circulation time of these aggregates by 7.6-fold. Moreover, under NIR stimulation, the nanofibers can effortlessly and rapidly convert into smaller nanoparticles without the need for additional groups, enabling deeper tumor penetration. The size-shrunken 1-NPs can infiltrate solid tumors effectively through photothermal effects, inhibiting tumor growth. Continuous monitoring of alterations in photoacoustic (PA) signals at distinct wavelengths using PA imaging identified the *in vivo* transformation from 1-NFs to 1-NPs in morphology. Hence, the NIR laser-induced, in-situ size transition from aza-BODIPY dye-1 into aza-BODIPY dye-1 with dual-state aggregation presented a robust treatment strategy for extended circulation and enhanced tumor penetration.

6.1. *Degradation strategy*

6.1.1. *Chemical bond break*

Wang et al.[118] illustrated a dendrimer-drug conjugate that penetrated deeply into PDA tumors *via* a cellular uptake mechanism and phagocytosis induced by γ-glutamyltransferase (GGT) (Fig. 8A). Using a ROS-sensitive linker, they covalently attached camptothecin (CPT) to polyamidoamine (PAMAM) dendrimers, followed by surface modification with glutathione to synthesize dendrimer-drug conjugates. Once delivered to the periphery of PDA tumors, the overexpression of GGT on vascular endothelial cells or tumor cells triggered the γ-glutamyl transfer reaction of glutathione, producing the original amine. The positively charged conjugate underwent rapid internalization through endocytosis mediated by vesicles and subsequent transcytosis, facilitating its deep penetration into the

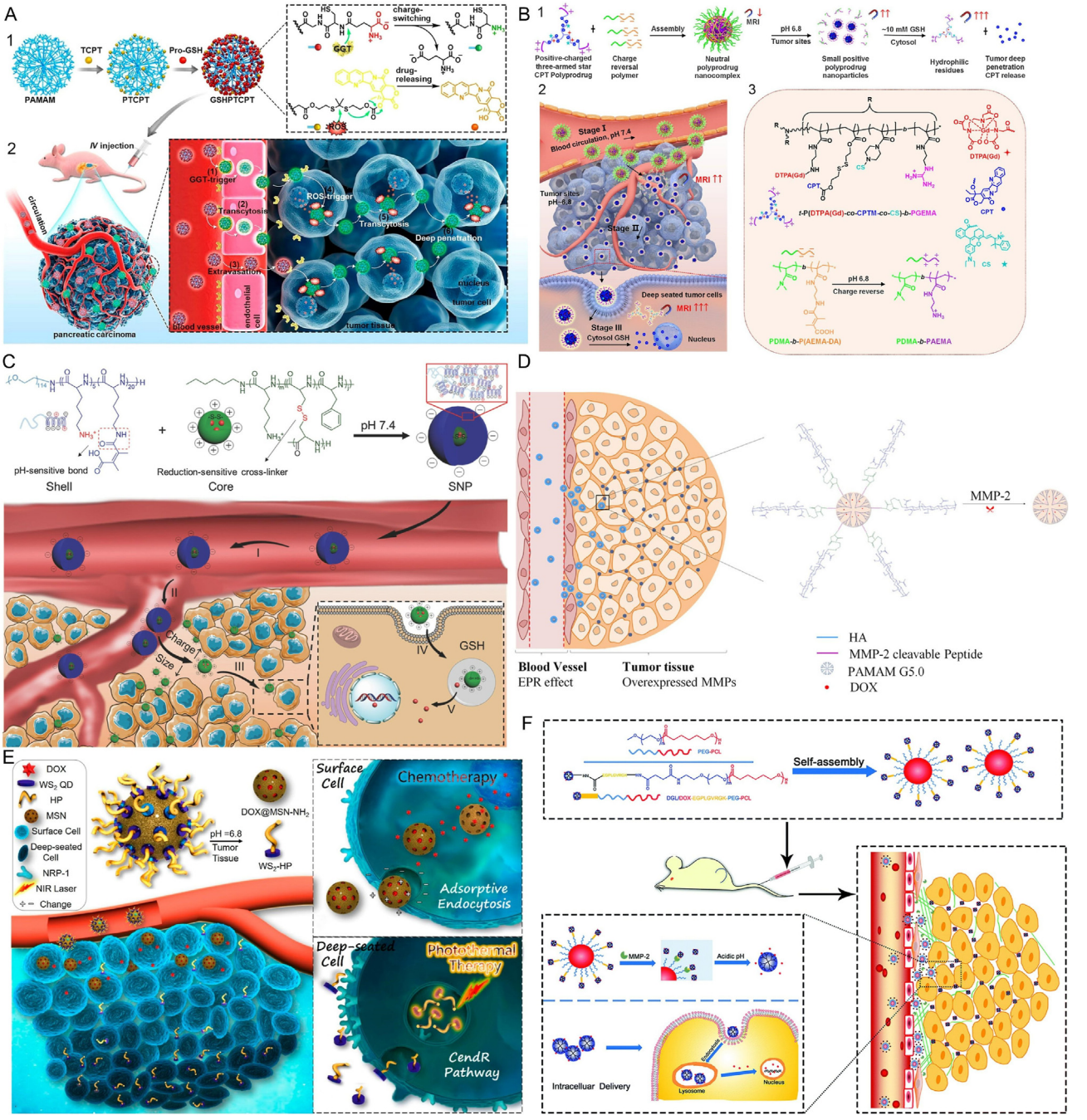

Figure 8 (A) Diagram illustrating the preparation of nanomedicines and the process of charge reversal catalyzed by GGT. 2. The positive charge is rapidly internalized *via* vesicle-mediated endocytosis, enhancing deep penetration into the tumor stroma. Reprinted with the permission from Ref. 118. Copyright © 2020 American Chemical Society. (B) Self-assembly and disassembly process of positively charged three-arm star-shaped multifunctional prodrug *t*-P(DTPA(Gd)-*co*-CPTM-*co*-CS)-*b*-PGEMA. 2. *In vivo* evaluation of SPNs for drug delivery with deep tumor penetration monitored through progressively enhanced magnetic resonance (MR) signals. 3. Structures of all polymers. Reprinted with the permission from Ref. 119. Copyright © 2020 American Chemical Society. (C) Shell-core nanoparticles (SNP) can achieve size reduction in reaction to the tumor's acidic pH. Reprinted with the permission from Ref. 120. Copyright © 2017 Wiley-VCH Verlag GmbH & Co. KGaA, Weinheim. (D) MMP-2 is highly expressed in the extracellular matrix of tumor cells, triggering the contraction of HA-pep-PAMAM from 200 to 10 nm, enabling its deep penetration into the tumor tissue. Reprinted with the permission from Ref. 121. Copyright © 2017 American Chemical Society. (E) Schematic illustration of the acid-labile nano-platform rapidly degrades into positively charged DOX@MSN-NH2 and small-sized WS2-HP, enhancing their tumor-penetrating abilities. Reprinted with the permission from Ref. 124. Copyright © 2017 American Chemical Society. (F) Accumulation and size reduction schematic of DGL/DOX@PP at the tumor site to surmount biological obstacles and penetrate deep into the tumor. Reprinted with the permission from Ref. 125. Copyright © 2018 The Royal Society of Chemistry.

tumor stroma. Following ROS cleavage inside cells, active CPT was released throughout the tumor. Compared to gemcitabine, the first-line chemotherapy drug used for the treatment of advanced pancreatic cancer, dendrimer−drug conjugates demonstrated superior anti-tumor activity in diverse mouse tumor models, including patient-derived pancreatic ductal adenocarcinoma (PDA) xenografts and *in situ* PDA tumor model.

Hao et al.[119] developed a stimuli-responsive multi-prodrug nanoparticles (SPNs), which were assembled from negatively charged coronas and positively charged multi-prodrug cores connected by disulfide bonds within the core, displaying a high payload of camptothecin (CPT). As shown in Fig. 8B, upon accumulation in tumor sites, SPNs disassembled to release small sizes of positively charged SPNs. These nanoparticles effectively infiltrated tumor cells, facilitating the release of substantial amounts of the parent CPT drug in the reducing cytoplasmic environment. Meanwhile, the multi-prodrug cores of SPNs, labeled with the magnetic resonance imaging contrast agent DTPA (Gd), served as a means to monitor the cascading degradation and biodistribution of SPNs, with the subsequent intracellular release of CPT. Size-switchable SPNs demonstrated noticeable tumor penetration and significant tumor suppression, making them promising candidates for precision diagnosis and treatment using endogenous activation.

6.1.2. *Onion peeling strategy*

The strategy of stripping the nanoparticle's outer shell layer to form smaller nanoparticles is referred to as the "onion-peeling" strategy. Recently, Chen et al.[120] developed shell-stacked nanoparticles (SNPs), which exhibited a significant size reduction in acidic tumor tissues (from ∼145 to 40 nm) with a surface charge reversal from −7.4 to 8.2 mV (Fig. 8C). This design aimed to boost the penetration and uptake of nanoparticles by cells in deep tumor tissue. The disulfide cross-linked core maintained particle stability, preventing undesired drug release until the outer shell was shed. This facilitated the cleavage of more exposed disulfide bonds, accelerating intracellular drug release. SNPs achieved a penetration depth of ∼1 mm in A549 lung cancer xenografts, which was ∼4-fold greater than in non-transformed lung cancer. SNPs loaded with DOX (SNP/DOX) exhibited a marked antitumor effect, nearly eliminating tumors, highlighting the significance of designing dual-transformable nanodrugs with changes in both size and charge. Han and colleagues[121] proposed a collapsible drug delivery system utilizing tumor microenvironment-responsive polysaccharide-modified dendrimers. As displayed in Fig. 8D, hyaluronic acid (HA) was attached to the surface amino groups of polyamidoamine (PAMAM) using an MMP-2-cleavable peptide (PLGLAG) *via* a click reaction. The initial size of these nanoparticles is ∼200 nm, but upon exposure to MMP-2, they underwent swift and substantial size alterations due to the cleavage of PLGLAG, which dissociated into their dendritic structural blocks (with a diameter of ∼10 nm). The rapid shrinkage promoted extravasation and accumulation of nanoparticles within tumors, improving their permeability and retention, thereby facilitating rapid diffusion and penetration of the nanoparticles.

6.1.3. *Surface-binding strategy*

The surface-binding strategy involves attaching small nanoparticles to the surface of large nanoparticles, creating a nanocomplex with a raspberry-like structure[122,123]. Within tumor tissues, the interconnected small nanoparticles can be quickly liberated as responsive ligands or molecules to the unique tumor microenvironment. Compared to the onion-like peeling strategy, surface drug loading can impart new functionalities to small nanodrugs, enhancing drug release rate and drug loading. Nevertheless, this also increased the intricacy of construction and preparation. Lei et al. devised a stimulus-responsive "Cluster Bomb" comprising mesoporous silica nanoparticles (MSN) adorned with penetrating and tumor-homing peptide-modified quantum dots (QDs) (Fig. 8E). Under normal physiological conditions, the azo bond, which acted as a linker between MSN and QDs, remained stable; however, it became markedly unstable under pH 6.8. Subsequently, the small-sized quantum dots can enhance tumor penetration and be used for photothermal therapy in deep tumors[124]. Cun et al.[125] constructed a size-switchable nano-platform based on an onion peeling strategy. This size-switchable nano-platform (DGL/DOX@PP) was produced by coupling small dendritic poly-L-lysine (DGL) with poly (ethylene glycol)-poly(ε-caprolactone) micelles using MMP-2-sensitive peptides (Fig. 8F). Initially, DGL/DOX@PP exhibited a nearly neutral charge and a size of 100 nm, enabling it to leverage the EPR effects. Following extravasation from tumor vasculature, DGL/DOX small nanoparticles responded to MMP-2 in the tumor microenvironment, rapidly releasing drugs from DGL/DOX@PP. The alteration in particle size significantly improved nanoparticle penetration into multicellular spheroids (MCSs) and tumors. Their results proved that size-switchable nano-platform outperformed small particles and non-switchable nanoparticles in suppressing tumor proliferation in 4T1 tumor-bearing mice. This adaptable nano-platform can offer a multifaceted strategy for modulating the tumor microenvironment and enhancing tumor penetration.

7. Reversible size-transformation

Research on reversible size-transformation aims to combine the benefits of both large nanoparticles and small nanoparticles for more efficient drug delivery, garnering increasing attention. Tumor microenvironment (TME)-responsive nanosystems represent a class of advanced nanomaterials designed for precise anticancer drug delivery[126]. Jia et al.[127] present an innovative size- and morphology-switchable nanodrug that responds to both the acidic TME and near-infrared (NIR) laser irradiation, with the goal of effective tumor destruction and inhibition of metastasis. The nanoagent comprises melittin (MEL), a cytolytic peptide; cypate, an NIR-absorbing molecule; and hyaluronic acid (HA), a tumor-targeting polymer. At a neutral pH of 7.4, the MEL/Cypate@HA complexes form negatively charged nanospheres (∼50 nm), ideal for prolonged systemic circulation. Upon reaching the tumor site, the acidic TME induces the transformation of these nanospheres into net-like nanofibers, which inhibit tumor cell movement and enhance the retention of the nanodrug for MEL-based chemotherapy. Additionally, NIR laser irradiation during cypate-mediated photothermal therapy degrades the nanofibers back into smaller nanospheres (∼25 nm), enabling deeper tumor penetration of MEL and leading to effective tumor eradication. Hypoxia, a common characteristic of most solid tumors, leads to significant resistance to chemotherapy and immunotherapy[128]. Wang et al.[129] introduce a tumor-acidity and bioorthogonal chemistry-mediated nanosystem designed to overcome hypoxic resistance and enhance chemo-immunotherapy. The system uses poly(2-azepane ethyl methacrylate), which responds rapidly to tumor acidity, and efficient bioorthogonal click chemistry to form large aggregates in tumor tissue, enhancing accumulation and retention. Another acidity-responsive group, maleic acid amide, responds more slowly, causing the aggregates to gradually dissociate into ultrasmall

nanoparticles. These nanoparticles penetrate the tumor more effectively, delivering doxorubicin (DOX) and nitric oxide (NO) to hypoxic tumor tissue, offering a novel strategy for enhanced tumor accumulation and penetration.

8. Major challenges of size transformable nanodrugs

While significant progress has been made in advancing size-transformable nanoparticles, numerous challenges remain, requiring further optimization and innovative solutions. First, there is the issue of off-target effects for internally triggered size-transformable nanosystem. The same stimuli that trigger size transformation could be present in other tissues, leading to undesired transformations and off-target adverse effects[29,130]. Therefore, developing nanosystems capable of accurately and specifically converting in target region are of considerable impact. Second, the protein corona could shield all the responsive components of nanodrugs. Once nanomedicines entered blood circulation, they will be quickly coated by the protein corona[131], masking responsive ligands (*e.g.*, enzymes and pH-responsive ligands) that are crucial for size-transformed nanodrug. Third, light can serve as a predominant external stimulus to regulate transformations. However, due to the limited tissue penetration capability of nanoparticles (NPs) within deep tissues[132], effectively regulating their size can be challenging. Therefore, there is an urgent need to explore innovative convertible nanosystems using alternative external stimuli with stronger tumor-penetrating capabilities, such as ultrasound, X-rays, and magnetic fields, to further fortify transformation within deep tissue. Fourth, the reactive time of the size-transformable nanoparticles in the tumor microenvironment is crucial. Due to the elevated interstitial pressure in tumor sites, nanoparticles entering the tumor region are susceptible to being expelled back into the blood vessels, yielding poor retention time[133]. Sensitivity and response time are critical factors in developing size-adjustable nanoparticles. As mentioned above, pH-triggered responses offer rapid and highly sensitive reactions, whereas the enzymatic reaction time with substrates may not be as swift. Enzyme-induced aggregation often occurs over a timeframe of 12−24 h, during which a considerable portion of the initial nanoparticles might be eliminated before aggregation initiates. Fifth, the intelligent design of size-transformable nanoparticles has the potential to remodel the tumor microenvironment[134], including the formation of extracellular matrix (ECM) structures like nanofibers. While such remodeling holds promise for enhancing drug delivery and efficacy, it also presents risks. Disruption and remodeling of the ECM can facilitate tumor migration and metastasis. Additionally, premature vascular normalization, resulting from this remodeling process, poses challenges for nanoparticles relying on passive tumor targeting through the enhanced permeability and retention (EPR) effect[135]. Achieving an optimal balance in both the degree and timing of microenvironment remodeling is therefore crucial to maximize the therapeutic benefits of size-transformable nanoparticles while mitigating unintended consequences.

9. Outlooks and future directions

Integrating the benefits of both large and small nano delivery systems has emerged as a promising strategy in cancer therapy. A plethora of approaches have been developed to create size-switchable nanocarriers responsive to diverse internal factors such as pH, enzymes, ROS, GSH, salts, lactate, and hypoxic environments as well as external stimuli like light and light-induced ROS/thermotherapy. These size-switchable nanotherapeutics, capable of adjusting their size under specific conditions, offer a range of advantages. They can enhance therapeutic efficacy by facilitating deep tumor penetration, prolonging retention times in targeted sites, controlling drug release, increasing intracellular uptake, reducing extracellular efflux, and even modifying or enhancing inherent physicochemical properties. Therefore, advancing innovation and creating more efficient nanocarriers are crucial for the future of nano-formulation development. Recently, smart transformable nanomedicines, capable of altering their physicochemical properties in response to internal and external stimuli, have emerged, offering the potential to overcome various barriers and enhance treatment efficacy. Additionally, there is increasing awareness that the substantial disparity between preclinical animal tumor models and clinical cancer patients profoundly affects the clinical translation of nano-formulations. Lastly, ensuring the scalability of production and the reproducibility of nanomedicines is essential for their clinical application. Here are the key points and challenges for future focus:

(1) Clinical translation discrepancy: Addressing the significant gap between findings in preclinical animal models and the realities of clinical cancer patients to enhance the clinical translation of nano-formulations.
(2) Scalability and reproducibility: Ensuring the ability to scale up production and maintain the reproducibility of nanomedicines for clinical application.
(3) Integration of dual strategies: Many existing size-transformable nanoparticles primarily focus on either size reduction or enlargement. Future designs should aim to integrate both strategies to optimize tumor penetration and prolong retention time at tumor sites.
(4) Simplicity in nanoparticle structure: Complex material structures may introduce additional variables, potentially obscuring the relationship between material properties and efficacy and limiting clinical application prospects. Therefore, future research and development should prioritize size-transformable materials with simple structures and excellent biocompatibility.

In conclusion, the size of nanoparticles plays a crucial role in enabling deep penetration and targeted delivery in cancer therapy. Therefore, careful consideration of the physicochemical properties and composition of nanoparticles is essential in the design of nanomedicines to achieve optimal antitumor effects. Moving forward, there is anticipation for the development of nanomedicines with straightforward structures, intelligent size-transformable capabilities, and high targeting efficiency, all of which hold promise for improving cancer therapy outcomes.

Acknowledgments

This work was supported in part by Startup and Retention Funds from the R. Ken Coit College of Pharmacy at The University of Arizona (UArizona), a PhRMA Foundation Faculty Starter Grant in Drug Delivery, UArizona Cancer Center Internal Pilot Award, and the National Institutes of Health (NIH) grants (R35GM147002 and R01CA272487).

Author contributions

Teng Ma: Conceptualization, Investigation, Writing − original draft, Writing − review & editing, Methodology, Visualization. Tuyen Ba Tran: Writing − review & editing. Ethan Lin: Writing − review & editing. Stephanie Hunt: Writing − review & editing. Riley Haveman: Writing − review & editing. Kylie Castro: Writing − review & editing. Jianqin Lu: Conceptualization, Funding acquisition, Project administration, Resources, Supervision, Writing − review & editing.

Conflicts of interest

The authors declare no conflict of interest.

References

1. Mitchell MJ, Billingsley MM, Haley RM, Wechsler ME, Peppas NA, Langer R. Engineering precision nanoparticles for drug delivery. *Nat Rev Drug Discov* 2021;**20**:101−24.
2. Sun T, Zhang YS, Pang B, Hyun DC, Yang M, Xia Y. Engineered nanoparticles for drug delivery in cancer therapy. *Angew Chem Int Ed* 2014;**53**:12320−64.
3. Gabizon A, Martin FJD. Polyethylene glycol-coated (pegylated) liposomal doxorubicin. *Drugs* 1997;**54**:15−21.
4. Socinski MA, Bondarenko I, Karaseva NA, Makhson AM, Vynnychenko I, Okamoto I, et al. Weekly nab-paclitaxel in combination with carboplatin *versus* solvent-based paclitaxel plus carboplatin as first-line therapy in patients with advanced non-small-cell lung cancer: final results of a phase III trial. *J Clin Oncol* 2012;**30**:2055−62.
5. Lu Y, Aimetti AA, Langer R, Gu Z. Bioresponsive materials. *Nat Rev Mater* 2016;**2**:16075.
6. Shi J, Kantoff PW, Wooster R, Farokhzad OC. Cancer nanomedicine: progress, challenges and opportunities. *Nat Rev Cancer* 2017;**17**:20−37.
7. Albanese A, Tang PS, Chan WC. The effect of nanoparticle size, shape, and surface chemistry on biological systems. *Annu Rev Biomed Eng* 2012;**14**:1−16.
8. Lee H, Hoang B, Fonge H, Reilly RM, Allen C. *In vivo* distribution of polymeric nanoparticles at the whole-body, tumor, and cellular levels. *Pharm Res* 2010;**27**:2343−55.
9. Cabral H, Matsumoto Y, Mizuno K, Chen Q, Murakami M, Kimura M, et al. Accumulation of sub-100 nm polymeric micelles in poorly permeable tumours depends on size. *Nat Nanotechnol* 2011;**6**:815−23.
10. Bai S, Zhang Y, Li D, Shi X, Lin G, Liu G. Gain an advantage from both sides: smart size-shrinkable drug delivery nanosystems for high accumulation and deep penetration. *Nano Today* 2021;**36**:101038.
11. Wang J, Mao W, Lock LL, Tang J, Sui M, Sun W, et al. The Role of micelle size in tumor accumulation, penetration, and treatment. *ACS Nano* 2015;**9**:7195−206.
12. Han X, Chen D, Sun J, Zhou J, Li D, Gong F, et al. A novel cabazitaxel-loaded polymeric micelle system with superior *in vitro* stability and long blood circulation time. *J Biomater Sci Polym Ed* 2016;**27**:626−42.
13. Yu W, Liu R, Zhou Y, Gao H. Size-tunable strategies for a tumor targeted drug delivery system. *ACS Cent Sci* 2020;**6**:100−16.
14. Carnovale C, Bryant G, Shukla R, Bansal V. Size, shape and surface chemistry of nano-gold dictate its cellular interactions, uptake and toxicity. *Prog Mater Sci* 2016;**83**:152−90.
15. Talamini L, Violatto MB, Cai Q, Monopoli MP, Kantner K, Krpetic Z, et al. Influence of size and shape on the anatomical distribution of endotoxin-free gold nanoparticles. *ACS Nano* 2017;**11**:5519−29.
16. Hashizume H, Baluk P, Morikawa S, McLean JW, Thurston G, Roberge S, et al. Openings between defective endothelial cells explain tumor vessel leakiness. *Am J Pathol* 2000;**156**:1363−80.
17. Moghimi SM, Hunter AC, Murray JC. Nanomedicine: current status and future prospects. *FASEB J* 2005;**19**:311−30.
18. Perrault SD, Walkey C, Jennings T, Fischer HC, Chan WCW. Mediating tumor targeting efficiency of nanoparticles through design. *Nano Lett* 2009;**9**:1909−15.
19. Sykes EA, Chen J, Zheng G, Chan WCW. Investigating the impact of nanoparticle size on active and passive tumor targeting efficiency. *ACS Nano* 2014;**8**:5696−706.
20. Luan S, Xie R, Yang Y, Xiao X, Zhou J, Li X, et al. Acid-responsive aggregated gold nanoparticles for radio sensitization and synergistic chemoradiotherapy in the treatment of esophageal cancer. *Small* 2022;**18**:2200115.
21. Liu R, Hu C, Yang Y, Zhang J, Gao H. Theranostic nanoparticles with tumor-specific enzyme-triggered size reduction and drug release to perform photothermal therapy for breast cancer treatment. *Acta Pharm Sin B* 2019;**9**:410−20.
22. Wang L, Huang J, Chen H, Wu H, Xu Y, Li Y, et al. Exerting enhanced permeability and retention effect driven delivery by ultrafine iron oxide nnanoparticles with T1−T2 switchable magnetic resonance imaging contrast. *ACS Nano* 2017;**11**:4582−92.
23. Poh S, Chelvam V, Low PS. Comparison of nanoparticle penetration into solid tumors and sites of inflammation: studies using targeted and nontargeted liposomes. *Nanomedicine* 2015;**10**:1439−49.
24. Wang R, Shen Q, Li X, Xie C, Lu W, Wang S, et al. Efficacy of inverso isomer of CendR peptide on tumor tissue penetration. *Acta Pharm Sin B* 2018;**8**:825−32.
25. Tang L, Yang X, Yin Q, Cai K, Wang H, Chaudhury I, et al. Investigating the optimal size of anticancer nanomedicine. *Proc Natl Acad Sci U S A* 2014;**111**:15344−9.
26. Maman S, Witz IP. A history of exploring cancer in context. *Nat Rev Cancer* 2018;**18**:359−76.
27. Ma K, Xu S, Tao T, Qian J, Cui Q, Su Rehman, et al. Magnetosome-inspired synthesis of soft ferrimagnetic nanoparticles for magnetic tumor targeting. *Proc Natl Acad Sci U S A* 2022;**119**:e2211228119.
28. Niu Y, Zhu J, Li Y, Shi H, Gong Y, Li R, et al. Size shrinkable drug delivery nanosystems and priming the tumor microenvironment for deep intratumoral penetration of nanoparticles. *J Control Release* 2018;**277**:35−47.
29. Zhou Y, Liu R, Shevtsov M, Gao H. When imaging meets size-transformable nanosystems. *Adv Drug Deliv Rev* 2022;**183**:114176.
30. Tong R, Chiang HH, Kohane DS. Photoswitchable nanoparticles for *in vivo* cancer chemotherapy. *Proc Natl Acad Sci U S A* 2013;**110**:19048−53.
31. Jia HR, Zhu YX, Liu X, Pan GY, Gao G, Sun W, et al. Construction of dually responsive nanotransformers with nanosphere−nanofiber−nanosphere transition for overcoming the size paradox of anticancer nanodrugs. *ACS Nano* 2019;**13**:11781−92.
32. Zhang X, Chen X, Guo Y, Jia HR, Jiang YW, Wu FG. Endosome/lysosome-detained supramolecular nanogels as an efflux retarder and autophagy inhibitor for repeated photodynamic therapy of multidrug-resistant cancer. *Nanoscale Horiz* 2020;**5**:481−7.
33. Mei L, Rao J, Liu Y, Li M, Zhang Z, He Q. Effective treatment of the primary tumor and lymph node metastasis by polymeric micelles with variable particle sizes. *J Control Release* 2018;**292**:67−77.
34. Gao Z, Hou Y, Zeng J, Chen L, Liu C, Yang W, et al. Tumor microenvironment-triggered aggregation of antiphagocytosis ^{99m}Tc-labeled Fe_3O_4 nanoprobes for enhanced tumor imaging *in vivo*. *Adv Mater* 2017;**29**:1701095.
35. Cheng X, Sun R, Yin L, Chai Z, Shi H, Gao M. Light-triggered assembly of gold nanoparticles for photothermal therapy and photoacoustic imaging of tumors *in vivo*. *Adv Mater* 2017;**29**:1604894.
36. Qi GB, Gao YJ, Wang L, Wang H. Self-assembled peptide-based nanomaterials for biomedical imaging and therapy. *Adv Mater* 2018;**30**:1703444.

37. Song N, Zhang Z, Liu P, Yang YW, Wang L, Wang D, et al. Nanomaterials with supramolecular assembly based on AIE luminogens for theranostic applications. *Adv Mater* 2020;**32**:2004208.
38. Ge W, Wang L, Zhang J, Ou C, Si W, Wang W, et al. Self-assembled nanoparticles as cancer therapeutic agents. *Adv Mater Inter* 2021;**8**:2001602.
39. Mi P, Miyata K, Kataoka K, Cabral H. Clinical translation of self-assembled cancer nanomedicines. *Adv Ther* 2021;**4**:2000159.
40. Sikder A, Esen C, O'Reilly RK. Nucleobase-interaction-directed biomimetic supramolecular self-assembly. *Acc Chem Res* 2022;**55**:1609−19.
41. Wen Y, Zhang W, Gong N, Wang YF, Guo HB, Guo W, et al. Carrier-free, self-assembled pure drug nanorods composed of 10-hydroxycamptothecin and chlorin e6 for combinatorial chemo-photodynamic antitumor therapy *in vivo*. *Nanoscale* 2017;**9**:14347−56.
42. Ren J, Zhang Z, Geng S, Cheng Y, Han H, Fan Z, et al. Molecular mechanisms of intracellular delivery of nanoparticles monitored by an enzyme-induced proximity labeling. *Nanomicro Lett* 2024;**16**:103.
43. Cao J, Yuan X, Sun X, Meng F, Li H, Hong Z, et al. Matrix metalloproteinase-2-induced morphologic transformation of self-assembled peptide nanocarriers inhibits tumor growth and metastasis. *ACS Mater Lett* 2023;**5**:900−8.
44. Zhang Y, He L, Wu J, Wang K, Wang J, Dai W, et al. Switchable PDT for reducing skin photosensitization by a NIR dye inducing self-assembled and photo-disassembled nanoparticles. *Biomaterials* 2016;**107**:23−32.
45. Zhang D, Qi GB, Zhao YX, Qiao SL, Yang C, Wang H. *In situ* formation of nanofibers from purpurin18-peptide conjugates and the assembly induced retention effect in tumor sites. *Adv Mater* 2015;**27**:6125−30.
46. Yuan Y, Wang L, Du W, Ding Z, Zhang J, Han T, et al. Intracellular self-assembly of taxol nanoparticles for overcoming multidrug resistance. *Angew Chem Int Edition* 2015;**54**:9700−4.
47. Ye D, Shuhendler AJ, Cui L, Tong L, Tee SS, Tikhomirov G, et al. Bioorthogonal cyclization-mediated *in situ* self-assembly of small-molecule probes for imaging caspase activity *in vivo*. *Nat Chem* 2014;**6**:519−26.
48. Paulsson J, Micke P. Prognostic relevance of cancer-associated fibroblasts in human cancer. *Semin Cancer Biol* 2014;**25**:61−8.
49. Zhao XX, Li LL, Zhao Y, An HW, Cai Q, Lang JY, et al. *In situ* self-assembled nanofibers precisely target cancer-associated fibroblasts for improved tumor imaging. *Angew Chem Int Ed* 2019;**58**:15287−94.
50. An HW, Li LL, Wang Y, Wang Z, Hou D, Lin YX, et al. A tumour-selective cascade activatable self-detained system for drug delivery and cancer imaging. *Nat Commun* 2019;**10**:4861.
51. Sharma U, Pal D, Prasad R. Alkaline phosphatase: an overview. *Indian J Clin Biochem* 2014;**29**:269−78.
52. Huang P, Gao Y, Lin J, Hao H, Liao H, Yan X, et al. Tumor-specific formation of enzyme-instructed supramolecular self-assemblies as cancer theranostics. *ACS Nano* 2015;**9**:9517−27.
53. Kato Y, Yamashita T, Ishikawa M. Relationship between expression of matrix metalloproteinase-2 and matrix metalloproteinase-9 and invasion ability of cervical cancer cells. *Oncol Rep* 2002;**9**:565−9.
54. Maurya SK, Poddar N, Tandon P, Yadav AK. Matrix metalloproteinases (MMPs) in cancer initiation and progression. In: Chakraborti S, Dhalla N, editors. *Pathophysiological aspects of proteases*. Singapore: Springer; 2017. p. 207−36.
55. Lee ES, Gao Z, Bae YH. Recent progress in tumor pH targeting nanotechnology. *J Control Release* 2008;**132**:164−70.
56. Gerweck LE. Tumor pH: implications for treatment and novel drug design. *Semin Radiat Oncol* 1998;**8**:176−82.
57. Tao Y, Liu S, Zhang Y, Chi Z, Xu J. A pH-responsive polymer based on dynamic imine bonds as a drug delivery material with pseudo target release behavior. *Polym Chem* 2018;**9**:878−84.
58. Moyer TJ, Finbloom JA, Chen F, Toft DJ, Cryns VL, Stupp SI. pH and amphiphilic structure direct supramolecular behavior in biofunctional assemblies. *J Am Chem Soc* 2014;**136**:14746−52.
59. Yang PP, Luo Q, Qi GB, Gao YJ, Li BN, Zhang JP, et al. Host materials transformable in tumor microenvironment for homing theranostics. *Adv Mater* 2017;**29**:1605869.
60. Han K, Zhang J, Zhang W, Wang S, Xu L, Zhang C, et al. Tumor-triggered geometrical shape switch of chimeric peptide for enhanced *in vivo* tumor internalization and photodynamic therapy. *ACS Nano* 2017;**11**:3178−88.
61. Wu K, Zowalaty AEE, Sayin VI, Papagiannakopoulos T. The pleiotropic functions of reactive oxygen species in cancer. *Nat Cancer* 2024;**5**:384−99.
62. Wu WS. The signaling mechanism of ROS in tumor progression. *Cancer Metastasis Rev* 2006;**25**:695−705.
63. Lee FYF, Vessey A, Rofstad E, Siemann DW, Sutherland RM. Heterogeneity of glutathione content in human ovarian cancer 1. *Cancer Res* 1989;**49**:5244−8.
64. Liu T, Lai L, Song Z, Chen T. A sequentially triggered nanosystem for precise drug delivery and simultaneous inhibition of cancer growth, migration, and invasion. *Adv Funct Mater* 2016;**26**:7775−90.
65. Yuan D, Ding L, Sun Z, Li X. MRI/Fluorescence bimodal amplification system for cellular GSH detection and tumor cell imaging based on manganese dioxide nanosheet. *Sci Rep* 2018;**8**:1747.
66. Bardwell JCA, McGovern K, Beckwith J. Identification of a protein required for disulfide bond formation *in vivo*. *Cell* 1991;**67**:581−9.
67. Guo WW, Zhang ZT, Wei Q, Zhou Y, Lin MT, Chen J, et al. Intracellular restructured reduced glutathione-responsive peptide nanofibers for synergetic tumor chemotherapy. *Biomacromolecules* 2020;**21**:444−53.
68. Sena Laura A, Chandel Navdeep S. Physiological roles of mitochondrial reactive oxygen species. *Mol Cell* 2012;**48**:158−67.
69. Yu T, Robotham JL, Yoon Y. Increased production of reactive oxygen species in hyperglycemic conditions requires dynamic change of mitochondrial morphology. *Proc Natl Acad Sci U S A* 2006;**103**:2653−8.
70. Zorov DB, Juhaszova M, Sollott SJ. Mitochondrial reactive oxygen species (ROS) and ROS-induced ROS release. *Physiol Rev* 2014;**94**:909−50.
71. Kirkinezos IG, Moraes CT. Reactive oxygen species and mitochondrial diseases. *Semin Cell Dev Biol* 2001;**12**:449−57.
72. Liang J, Liu B. ROS-responsive drug delivery systems. *Bioeng Transl Med* 2016;**1**:239−51.
73. Cheng DB, Zhang XH, Gao YJ, Ji L, Hou D, Wang Z, et al. Endogenous reactive oxygen species-triggered morphology transformation for enhanced cooperative interaction with mitochondria. *J Am Chem Soc* 2019;**141**:7235−9.
74. Shamsipur M, Ghavidast A, Pashabadi A. Phototriggered structures: latest advances in biomedical applications. *Acta Pharm Sin B* 2024;**13**:2844−76.
75. Shen L, Zhou T, Fan Y, Chang X, Wang Y, Sun J, et al. Recent progress in tumor photodynamic immunotherapy. *Chin Chem Lett* 2020;**31**:1709−16.
76. Kim MS, Diamond SL. Photocleavage of *o*-nitrobenzyl ether derivatives for rapid biomedical release applications. *Bioorg Med Chem Lett* 2006;**16**:4007−10.
77. Kopke T, Zaleski JM. Diazo-containing molecular constructs as potential anticancer agents: from diazo[b]fluorene natural products to photoactivatable diazo-oxochlorins. *Anti Cancer Agents Med Chem* 2008;**8**:292−304.
78. Webber MJ, Newcomb CJ, Bitton R, Stupp SI. Switching of self-assembly in a peptide nanostructure with a specific enzyme. *Soft Matter* 2011;**7**:9665−72.
79. Kundu PK, Samanta D, Leizrowice R, Margulis B, Zhao H, Börner M, et al. Light-controlled self-assembly of non-photoresponsive nanoparticles. *Nat Chem* 2015;**7**:646−52.
80. Pieroni O, Fissi A, Angelini N, Lenci F. Photoresponsive polypeptides. *Acc Chem Res* 2001;**34**:9−17.

81. Cheng X, Sun R, Yin L, Chai Z, Shi H, Gao M. Light-triggered assembly of gold nanoparticles for photothermal therapy and photoacoustic imaging of tumors *In vivo*. *Adv Mater* 2017;**29**:27921316.
82. Liu R, An Y, Jia W, Wang Y, Wu Y, Zhen Y, et al. Macrophage-mimic shape changeable nanomedicine retained in tumor for multimodal therapy of breast cancer. *J Control Release* 2020;**321**:589−601.
83. Ma T, Chen R, Lv N, Li Y, Yang ZR, Qin H, et al. Morphological transformation and *in situ* polymerization of caspase-3 responsive diacetylene-containing lipidated peptide amphiphile for self-amplified cooperative antitumor therapy. *Small* 2022;**18**:e2204759.
84. Wang Z, An HW, Hou D, Wang M, Zeng X, Zheng R, et al. Addressable peptide self-assembly on the cancer cell membrane for sensitizing chemotherapy of renal cell carcinoma. *Adv Mater* 2019;**31**:1807175.
85. Liu Y, Yu Y, Lam JWY, Hong Y, Faisal M, Yuan WZ, et al. Simple biosensor with high selectivity and sensitivity: thiol-specific biomolecular probing and intracellular imaging by AIE fluorogen on a TLC plate through a thiol−ene click mechanism. *Chem Eur J* 2010;**16**:8433−8.
86. Ai X, Ho CJH, Aw J, Attia ABE, Mu J, Wang Y, et al. *In vivo* covalent cross-linking of photon-converted rare-earth nanostructures for tumour localization and theranostics. *Nat Commun* 2016;**7**:10432.
87. Xie R, Ruan S, Liu J, Qin L, Yang C, Tong F, et al. Furin-instructed aggregated gold nanoparticles for re-educating tumor associated macrophages and overcoming breast cancer chemoresistance. *Biomaterials* 2021;**275**:120891.
88. Ruan S, Hu C, Tang X, Cun X, Xiao W, Shi K, et al. Increased gold nanoparticle retention in brain tumors by *in situ* enzyme-induced aggregation. *ACS Nano* 2016;**10**:10086−98.
89. Elsabahy M, Wooley KL. Design of polymeric nanoparticles for biomedical delivery applications. *Chem Soc Rev* 2012;**41**:2545−61.
90. Rodrigues S, Costa AMRd, Grenha A. Chitosan/carrageenan nanoparticles: effect of cross-linking with tripolyphosphate and charge ratios. *Carbohydr Polym* 2012;**89**:282−9.
91. Hung CC, Huang WC, Lin YW, Yu TW, Chen HH, Lin SC, et al. Active tumor permeation and uptake of surface charge-switchable theranostic nanoparticles for imaging-guided photothermal/chemo combinatorial therapy. *Theranostics* 2016;**6**:302−17.
92. Nam J, Won N, Jin H, Chung H, Kim S. pH-Induced aggregation of gold nanoparticles for photothermal cancer therapy. *J Am Chem Soc* 2009;**131**:13639−45.
93. Zhang Y, Huang F, Ren C, Liu J, Yang L, Chen S, et al. Enhanced radiosensitization by gold nanoparticles with acid-triggered aggregation in cancer radiotherapy. *Adv Sci* 2019;**6**:1801806.
94. Gentili D, Guido O. Reversible assembly of nanoparticles: theory, strategies and computational simulations. *Nanoscale* 2022;**14**:14385−432.
95. Sun M, Liu F, Zhu Y, Wang W, Hu J, Liu J, et al. Salt-induced aggregation of gold nanoparticles for photoacoustic imaging and photothermal therapy of cancer. *Nanoscale* 2016;**8**:4452−7.
96. Zhang YR, Lin R, Li HJ, He Wl, Du JZ, Wang J. Strategies to improve tumor penetration of nanomedicines through nanoparticle design. *Wires Nanomed Nanobi* 2019;**11**:e1519.
97. Li Z, Shan X, Chen Z, Gao N, Zeng W, Zeng X, et al. Applications of surface modification technologies in nanomedicine for deep tumor penetration. *Adv Sci* 2021;**8**:2002589.
98. Panté N, Kann M. Nuclear pore complex is able to transport macromolecules with diameters of ∼39 nm. *Mol Biol Cel* 2002;**13**:425−34.
99. Souri M, Soltani M, Moradi Kashkooli F, Kiani Shahvandi M. Engineered strategies to enhance tumor penetration of drug-loaded nanoparticles. *J Control Release* 2022;**341**:227−46.
100. Soo Choi H, Liu W, Misra P, Tanaka E, Zimmer JP, Itty Ipe B, et al. Renal clearance of quantum dots. *Nat Biotechnol* 2007;**25**:1165−70.
101. Chen KH, Lundy DJ, Toh EKW, Chen CH, Shih C, Chen P, et al. Nanoparticle distribution during systemic inflammation is size-dependent and organ-specific. *Nanoscale* 2015;**7**:15863−72.
102. Sun J, Li J, Li X, Yang L, Liu Y, Gao H, et al. Sequentially responsive size reduction and drug release of core-satellite nanoparticles to enhance tumor penetration and effective tumor suppression. *Chin Chem Lett* 2023;**34**:107891.
103. Mai Y, Eisenberg A. Self-assembly of block copolymers. *Chem Soc Rev* 2012;**41**:5969−85.
104. Pijpers IAB, Abdelmohsen LKEA, Williams DS, van Hest JCM. Morphology under control: engineering biodegradable stomatocytes. *ACS Macro Lett* 2017;**6**:1217−22.
105. Williams DS, Pijpers IAB, Ridolfo R, van Hest JCM. Controlling the morphology of copolymeric vectors for next generation nanomedicine. *J Control Release* 2017;**259**:29−39.
106. Cao S, Abdelmohsen LKEA, Shao J, van den Dikkenberg J, Mastrobattista E, Williams DS, et al. pH-Induced transformation of biodegradable multilamellar nanovectors for enhanced tumor penetration. *ACS Macro Lett* 2018;**7**:1394−9.
107. Kozin SV, Shkarin P, Gerweck LE. The cell transmembrane pH gradient in tumors enhances cytotoxicity of specific weak acid chemotherapeutics. *Cancer Res* 2001;**61**:4740−3.
108. Li HJ, Du JZ, Du XJ, Xu CF, Sun CY, Wang HX, et al. Stimuli-responsive clustered nanoparticles for improved tumor penetration and therapeutic efficacy. *Proc Natl Acad Sci U S A* 2016;**113**:4164−9.
109. Zhang Z, Wang T, Yang R, Fu S, Guan L, Hou T, et al. Small morph nanoparticles for deep tumor penetration *via* caveolae-mediated transcytosis. *ACS Appl Mater Inter* 2020;**12**:38499−511.
110. Helmlinger G, Yuan F, Dellian M, Jain RK. Interstitial pH and pO_2 gradients in solid tumors *in vivo*: high-resolution measurements reveal a lack of correlation. *Nat Med* 1997;**3**:177−82.
111. Ma T, Chen R, Lv N, Chen Y, Qin H, Jiang H, et al. Size-transformable bicomponent peptide nanoparticles for deep tumor penetration and photo-chemo combined antitumor therapy. *Small* 2022;**18**:e2106291.
112. Kennedy L, Sandhu JK, Harper M-E, Cuperlovic-Culf M. Role of glutathione in cancer: from mechanisms to therapies. *Biomolecules* 2020;**10**:1429.
113. Xiong Y, Xiao C, Li Z, Yang X. Engineering nanomedicine for glutathione depletion-augmented cancer therapy. *Chem Soc Rev* 2021;**50**:6013−41.
114. Guo X, Wei X, Jing Y, Zhou S. Size Changeable nanocarriers with nuclear targeting for effectively overcoming multidrug resistance in cancer therapy. *Adv Mater* 2015;**27**:6450−6.
115. Wang H, Li Y, Bai H, Shen J, Chen X, Ping Y, et al. A cooperative dimensional strategy for enhanced nucleus-targeted delivery of anticancer drugs. *Adv Funct Mater* 2017;**27**:1700339.
116. Zhang Y, Du X, Liu S, Yan H, Ji J, Xi Y, et al. NIR-triggerable ROS-responsive cluster-bomb-like nanoplatform for enhanced tumor penetration, phototherapy efficiency and antitumor immunity. *Biomaterials* 2021;**278**:121135.
117. Chen Y, Zhang XH, Cheng DB, Zhang Y, Liu Y, Ji L, et al. Near-infrared laser-triggered *in situ* dimorphic transformation of BF_2-azadipyrromethene nanoaggregates for enhanced solid tumor penetration. *ACS Nano* 2020;**14**:3640−50.
118. Wang G, Zhou Z, Zhao Z, Li Q, Wu Y, Yan S, et al. Enzyme-triggered transcytosis of dendrimer−drug conjugate for deep penetration into pancreatic tumors. *ACS Nano* 2020;**14**:4890−904.
119. Hao Q, Wang Z, Zhao W, Wen L, Wang W, Lu S, et al. Dual-responsive polyprodrug nanoparticles with cascade-enhanced magnetic resonance signals for deep-penetration drug release in tumor therapy. *ACS Appl Mater Inter* 2020;**12**:49489−501.
120. Chen J, Ding J, Wang Y, Cheng J, Ji S, Zhuang X, et al. Sequentially responsive shell-stacked nanoparticles for deep penetration into solid tumors. *Adv Mater* 2017;**29**:1701170.
121. Han M, Huang-Fu MY, Guo WW, Guo NN, Chen J, Liu HN, et al. MMP-2-sensitive HA end-conjugated poly(amidoamine) dendrimers

via click reaction to enhance drug penetration into solid tumor. *ACS Appl Mater Inter* 2017;**9**:42459−70.
122. Li J, Ke W, Li H, Zha Z, Han Y, Ge Z. Endogenous stimuli-sensitive multistage polymeric micelleplex anticancer drug delivery system for efficient tumor penetration and cellular internalization. *Adv Healthc Mater* 2015;**4**:2206−19.
123. Ruan S, Cao X, Cun X, Hu G, Zhou Y, Zhang Y, et al. Matrix metalloproteinase-sensitive size-shrinkable nanoparticles for deep tumor penetration and pH triggered doxorubicin release. *Biomaterials* 2015;**60**:100−10.
124. Lei Q, Wang SB, Hu JJ, Lin YX, Zhu CH, Rong L, et al. Stimuli-responsive "cluster bomb" for programmed tumor therapy. *ACS Nano* 2017;**11**:7201−14.
125. Cun X, Li M, Wang S, Wang Y, Wang J, Lu Z, et al. A size switchable nanoplatform for targeting the tumor microenvironment and deep tumor penetration. *Nanoscale* 2018;**10**:9935−48.
126. Li M, Ning Y, Chen J, Duan X, Song N, Ding D, et al. Proline isomerization-regulated tumor microenvironment adaptable self-assembly of peptides for enhanced therapeutic efficacy. *Nano Lett* 2019;**19**:7965−76.
127. Jia H, Zhu Y, Liu X, Pan G, Gao G, Sun W, et al. Construction of dually responsive nanotransformers with nanosphere−nanofiber−nanosphere transition for overcoming the size paradox of anticancer nanodrugs. *ACS Nano* 2019;**13**:11781−92.
128. Xin X, Kumar V, Lin F, Kumar V, Bhattarai R, Bhatt VR, et al. Redox-responsive nanoplatform for codelivery of miR-519c and gemcitabine for pancreatic cancer therapy. *Sci Adv* 2020;**6**:eabd6764.
129. Wang K, Jiang M, Zhou J, Liu Y, Zong Q, Yuan Y. Tumor-acidity and biorthogonal chemistry mediated on-site size transformation clustered nanosystem to overcome hypoxic resistance and enhance chemoimmunotherapy. *ACS Nano* 2022;**16**:721−35.
130. Zhou Q, Xiang J, Qiu N, Wang Y, Piao Y, Shao S, et al. Tumor abnormality-oriented nanomedicine design. *Chem Rev* 2023;**123**:10920−89.
131. Xiao W, Gao H. The impact of protein corona on the behavior and targeting capability of nanoparticle-based delivery system. *Int J Pharmaceut* 2018;**552**:328−39.
132. Jiang S, Huang K, Qu J, Lin J, Huang P. Cancer nanotheranostics in the second near-infrared window. *View* 2021;**2**:20200075.
133. Nichols JW, Bae YH. Odyssey of a cancer nanoparticle: from injection site to site of action. *Nano Today* 2012;**7**:606−18.
134. Guo Q, He X, Li C, He Y, Peng Y, Zhang Y, et al. Dandelion-like tailorable nanoparticles for tumor microenvironment modulation. *Adv Sci* 2019;**6**:1901430.
135. Overchuk M, Zheng G. Overcoming obstacles in the tumor microenvironment: recent advancements in nanoparticle delivery for cancer theranostics. *Biomaterials* 2018;**156**:217−37.